LAHO

otes

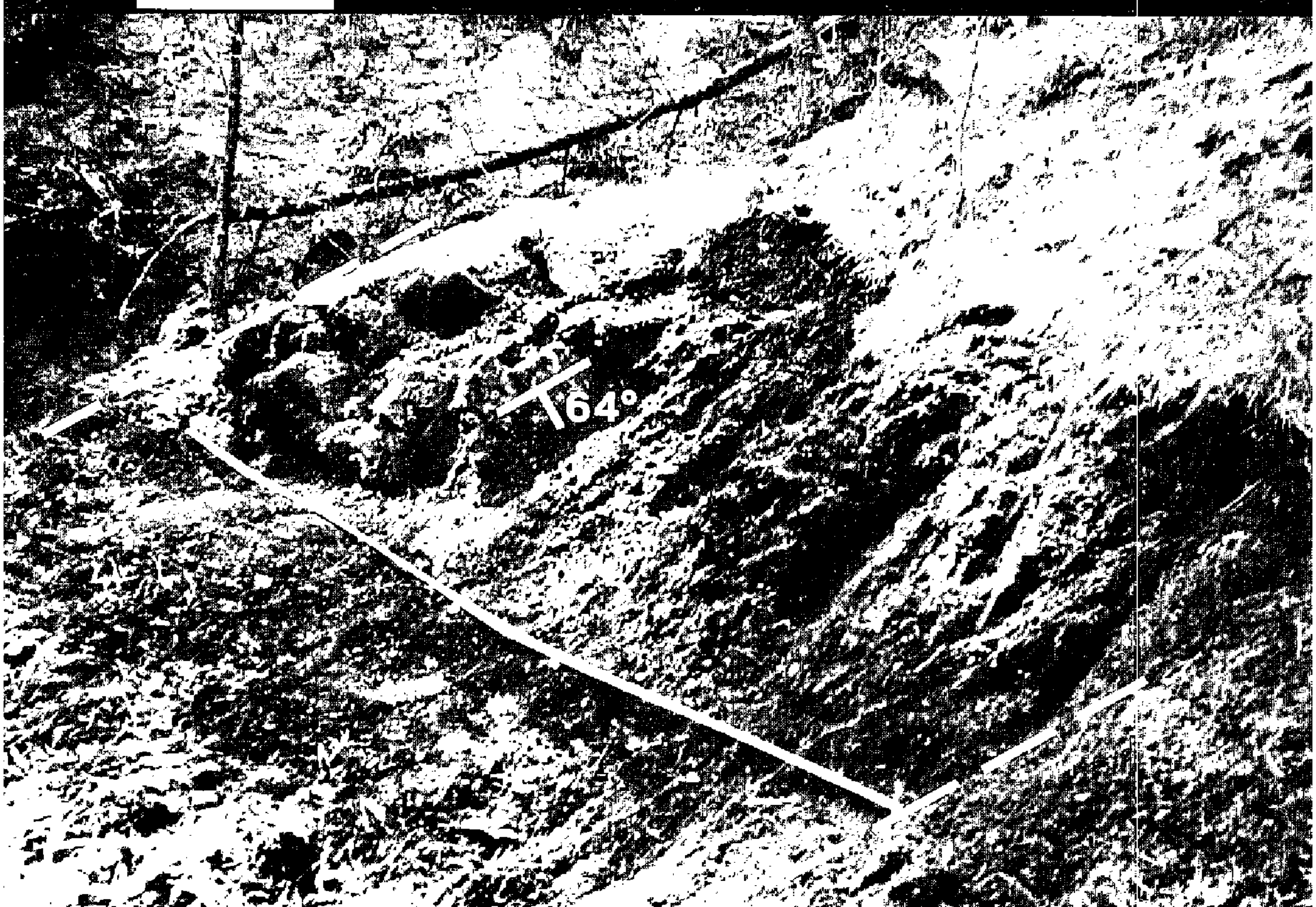

April 1999
Vol. 59, No. 2

On The Cover —

Hartshorne Coal Bed, Latimer County—Thickest Known Coal in Oklahoma

A 10-ft-thick bituminous coal bed exposed in the NW¼NW¼SW¼NE¼ sec. 35, T. 6 N., R. 18 E., Latimer County, is the thickest known occurrence of coal in the State. The coal bed is exposed at the west end of an abandoned pit in an area where the dip of the strata is too steep (64°) for strip mining. (The steep dip of the coal bed is well shown at the edge of a narrow gully [inset photo, p. 78] just below the measured exposure.) The thickness of the coal was computed from the formula $T = H \sin d$, where T is the stratigraphic thickness, H is the horizontal distance across the bed measured perpendicular to the strike, and d is the angle of dip. (T = 11.8 ft × 0.848, or thickness = 10.02 ft).

The atypical thickness of the coal is due to the convergence of the 6-ft-thick Lower Hartshorne coal bed and the 4-ft-thick Upper Hartshorne coal bed. A 0.5-in.-thick carbonaceous shale parting separates the two coals. However, the 10-ft-thick occurrence is correctly identified as a single bed, called the Hartshorne coal. Where noncoal material in a parting does not exceed the thickness of the coal in either the underlying or overlying benches, the coal is considered a single bed (Wood and others, 1983, p. 36).

Russell (1960, p. 12) discussed the coalescence of Upper and Lower Hartshorne coal beds in the same area. He measured a section in the C N½ sec. 35, T. 6 N., R. 18 E., and stated that the coal beds "are separated by a 0.5-foot carbonaceous shale and measure 10 feet in the aggregate." Wilson (1970, p. 304–305) studied the paly-

(continued on p. 78)

OKLAHOMA GEOLOGY NOTES, ISSN 0030-1736, is published bimonthly by the Oklahoma Geological Survey. It contains short technical articles, mineral-industry and petroleum news and statistics, abstracts, notices of new publications, and announcements of general pertinence to Oklahoma geology. Single copies, $1.50; yearly subscription, $6. Send subscription orders to the Survey at 100 E. Boyd, Room N-131, Norman, OK 73019. Short articles on aspects of Oklahoma geology are welcome from contributors; general guidelines will be sent on request.

This publication, printed by the Oklahoma Geological Survey, Norman, Oklahoma, is issued by the Oklahoma Geological Survey as authorized by Title 70, Oklahoma Statutes 1981, Section 3310, and Title 74, Oklahoma Statutes 1981, Sections 231–238. 1,500 copies have been prepared for distribution at a cost of $1314 to the taxpayers of the State of Oklahoma. Copies have been deposited with the Publications Clearinghouse of the Oklahoma Department of Libraries.

OKLAHOMA GEOLOGY

Notes

April 1999
VOL. 59, NO. 2

Interpretation of Surface and Subsurface Gamma-Ray Profiles, Hartshorne Formation, Arkoma Basin, Southeastern Oklahoma

Richard D. Andrews[1] *and Neil H. Suneson*[1]

Abstract

During the fall and spring of 1998–99, gamma-ray profiles were recorded at six localities where the Hartshorne Formation is exposed. The Hartshorne Formation consists predominantly of sandstone and shale, and gamma-ray profiling is demonstrably useful in distinguishing between these rock types. The profiles were made in conjunction with a workshop and field trip sponsored by the Oklahoma Geological Survey and the Petroleum Technology Transfer Council.

The purpose of this study was to compare gamma-ray profiles of measured sections to wireline well logs and to predict subsurface depositional environments and rock types by comparison to surface exposures. Gamma-ray profiles representing the six outcrop localities clearly distinguished between the main rock types indigenous to the formations studied: sandstone, shale, coal, and shaly sandstone layers. Textural variations—i.e., the relative grain sizes of clastic sequences—were also clearly identified from the gamma-ray profiles and reflect the amount of interbedded shale and interstitial clay.

Because depositional environments of rock units at the surface can be interpreted, their gamma-ray profiles can be compared to similar measurements recorded on subsurface wireline logs. The responses shown on these logs can then be related to the responses taken at the surface. Thus, better interpretations can be made from wireline logs regarding depositional environments, rock types, and reservoir quality.

Introduction

The gamma-ray profiles described in this study resulted from a field trip and workshop on the Hartshorne Formation conducted in late 1998. One emphasis of the field trip was to compare rock types, textural variations, and depositional environments of Hartshorne outcrops to those shown on subsurface wireline well logs. The outcrop-to-log comparisons are included in Oklahoma Geological Survey Guidebook 31 (Suneson, 1998), which is a companion publication to the workshop publication (Andrews and others, 1998). In order to verify the outcrop-to-log relationship, it was necessary to measure the gamma radiation of surface exposures where the rock types and textural variations are known and depositional environments could be interpreted. The wireline gamma-ray well logs could then be compared to the measured surface gamma-ray profiles. The similarity of surface and subsurface gamma-ray logs enables interpretations of depositional environments and rock types to be made using wireline gamma-ray logs.

Gamma-ray profiles are made from surface gamma-radiation measurements that are plotted in a vertical log format using graphing software such as MS Excel. Gamma-ray profiles generally measure the relative abundance of interbedded

[1]Oklahoma Geological Survey.

shale or interstitial clay, both of which produce relatively large amounts of gamma radiation compared to other common sedimentary rocks such as sandstone, limestone, or coal. Therefore, the gamma-ray profile (or wireline log) can be used to distinguish between these rock types. Generally speaking, sandstone with little interstitial clay or interbedded shale exhibits low gamma-ray values and is called *clean*. Sandstone having larger amounts of interstitial clay and interbedded shale can be called *dirty* and have gamma-ray values between those of a clean sandstone and a shale.

For this study, outcrops were selected to represent specific, clearly defined lithofacies. In addition, the outcrops are well exposed and have little ground cover. The exposures comprise simple depositional sequences that can be interpreted with a fair degree of certainty. The gamma-ray profiles made from these exposures can therefore be interpreted and compared to gamma-ray logs from oil and gas wells.

Previous Studies

Hartshorne Formation

The Desmoinesian Hartshorne Formation in Oklahoma is the lowest formation of the Krebs Group, which also includes, in ascending order, the McAlester, Savanna, and Boggy Formations. The Hartshorne is exposed from near Morrilton, Arkansas, on the east, to Harden City, Oklahoma, on the west, to Muskogee, Oklahoma, on the north (Hemish and Suneson, 1997). In Oklahoma, the northern and southern exposures reflect the margins of the Arkoma basin. The Hartshorne Formation is buried by younger strata throughout much of the basin, and its western extent in the subsurface extends onto the Cherokee platform.

Early studies of the Hartshorne Formation focused on its coal resources. Hendricks and others (1936, p. 1348) noted that parts of the Hartshorne are marine and other parts are "continental or lacustrine." Scruton (1950, p. 424) was the first to apply the term *deltaic* to surface exposures of the Hartshorne Formation, and Houseknecht and others (1983, 1984) interpreted the Hartshorne in the subsurface in terms of a delta model. Andrews and others (1998) reviewed the hydrocarbon-production history of the Hartshorne in the Arkoma basin and documented marine (prodelta, distributary-mouth-bar), fluvial (channel, distributary-channel), and overbank (crevasse-splay, bay-fill) facies throughout the area, based on interpretation of wireline logs, cores, and outcrops. Recent workers generally agree that the sediment in the formation was derived mostly from the east.

The Hartshorne Formation is a prolific producer of natural gas and was an important source of coal. Andrews and others (1998) estimated that more than 675 billion cubic feet of gas has been produced from the Hartshorne through 1997. Most of the gas is produced from relatively thick channel-fill sandstones, although some is produced from thinner marine sandstones. Methane is produced from the Hartshorne coal primarily in the eastern part of the Arkoma basin in Oklahoma. The first coal from the Hartshorne Formation was mined in 1872; at present, only one underground mine is currently mining Hartshorne coal in Oklahoma.

Delta Systems

This paper follows the model of a delta system described by Coleman and Prior (1982). As summarized by Andrews (1995, p. 4–10):

> A delta is defined as an accumulation of river-derived sediment that is deposited as an extension to the coast. . . . The basic components of a prograding delta system . . . include the upper delta plain, lower delta plain, subaqueous delta or delta front . . . and prodelta. . . . The upper delta plain extends from the down-flow edge of the coastal flood plain to the limit of effective tidal inundation of the lower delta plain. The upper delta plain essentially is the portion of a delta that is unaffected by marine processes. Recognizable depositional environments in the upper delta plain include meandering rivers, distributary channels, lacustrine delta-fill, extensive swamps and marshes, and fresh-water lakes. . . . In the lower delta plain, sediments are influenced highly by marine conditions, which extend from the subaqueous delta front to the landward limit of marine (tidal) influence. . . . The lower delta plain consists primarily of bay-fill deposits [including crevasse-splay sands], which occur between or adjacent to major distributaries, and secondarily of distributary-channel deposits. Distributary mouth bars and bar-finger deposits are the principal components of the subaqueous delta front.

Each part of a delta generally consists of a distinctive sequence of rock types. For example, distributary-mouth bars typically consist of a gradationally coarsening (or "cleaning") upward sequence of shale, siltstone, and sandstone. Delta-plain environments typically contain coal. Channels generally contain thick accumulations of sandstone and exhibit abrupt bases. As a result, the different deltaic environments can be interpreted from outcrops and wireline logs (Figs. 1,2). In Oklahoma, lower- and upper-delta-plain, delta-front, and prodelta environments have been recognized in the Hartshorne Formation. In addition, the principal reservoir rock in the central part of the Arkoma basin occurs in low-stand incised fluvial channels.

Gamma-Ray Profiles

Introduction and Principles

Gamma rays are produced from the decay of naturally occurring radioactive isotopes in rocks. The most common radioactive elements are uranium, thorium, and an isotope of potassium. Most feldspars and clay minerals contain some potassium and thorium, and these radioactive isotopes produce most of the gamma radiation associated with typical marine shales. In contrast, sandstone with a high quartz content usually contains relatively little potassium or thorium and therefore gives off little gamma radiation. These observations mean that gamma-ray profiles, either from wells or surface exposures, can be related in a general way to the rock types or textural profile of a stratigraphic interval. (*Textural profile* in this report refers to clastic grain-size distribution.) Although it is not possible to quantify clastic-grain size, a reasonable interpretation of detrital composition—i.e., clay, silt, and sand—can be made from gamma-ray profiles. Exceptions to this, of course, do occur, such as in sandstone containing radioactive elements like uranium or abundant potassium feldspar. These occurrences are rare, and radioactive sandstone typically can be identified by using gamma-ray logs with other wireline logs.

Typical Gamma-Ray Responses

Most common clastic sequences are characterized by variable amounts of shale. The amount of shale and its relation to any interbedded sandstone generally are caused by variations in depositional processes that, in turn, characterize specific

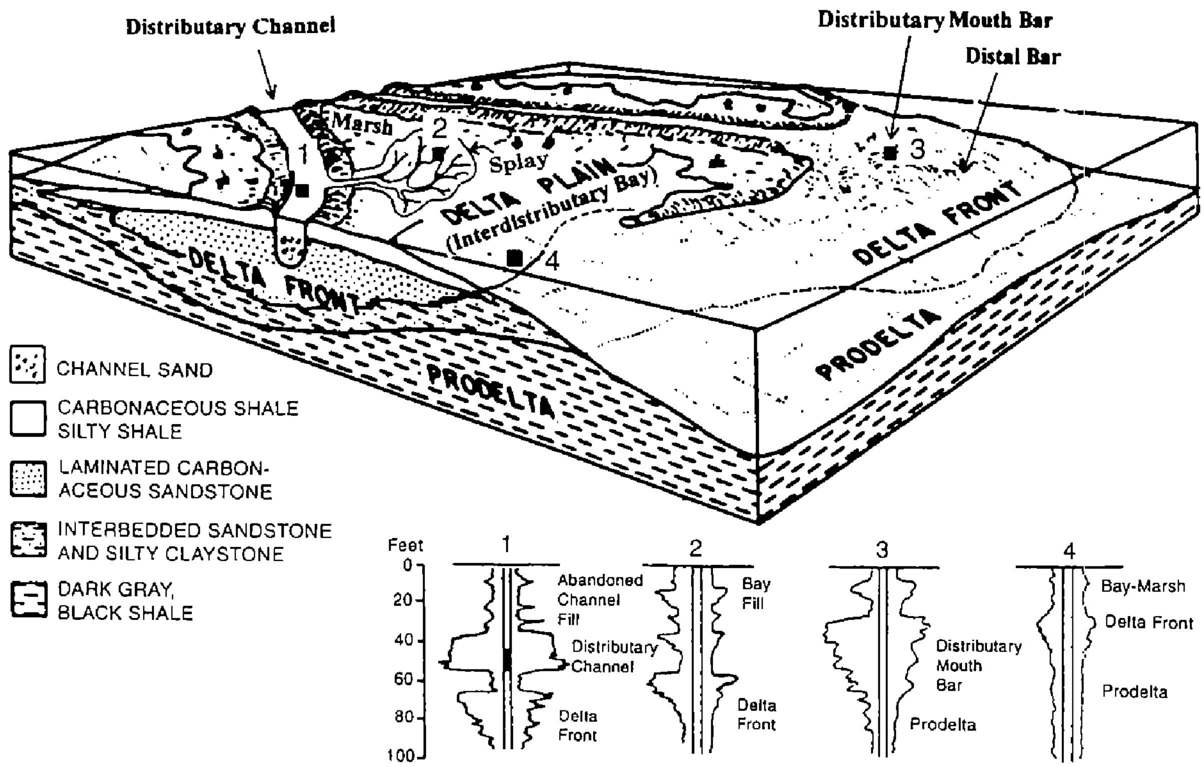

Figure 1. Schematic model of deltaic depositional environments. Idealized electric-log responses and interpreted facies are shown for locations 1–4. Modified from Brown (1979).

clastic facies. Gamma-ray profiles, which "measure" the amount of shale in a clastic sequence, can therefore be useful in identifying particular lithofacies (e.g., Howe, 1989; Jordan and others, 1991; Slatt and others, 1995). In many cases, a gamma-ray profile is not diagnostic of a particular lithofacies, but it can be used to eliminate certain possibilities. This is particularly true in basins where (1) the gamma-ray profiles of different formations are well established, (2) there is adequate coverage by gamma-ray logs, and (3) surface outcrops provide additional information not available on logs.

For example, sediments in fluvial channels ("point bar" in Fig. 2) are deposited during different processes that can be identified in outcrop and interpreted from gamma-ray logs. The lower part of a channel deposit typically contains thick, relatively clean sand that exhibits high-angle cross-bedding or is unstratified due to high energy and rapid deposition. Higher in the channel sequence, sand beds become thinner, and the grain size usually decreases, reflecting lower water velocities and less-rapid sediment deposition as the channel fills. In the upper part of a channel sequence, sediments typically consist of interbedded sand and mud. The amount of sand decreases as the channel is abandoned (different process), and the sequence becomes mostly mud and silt. The gamma-ray profile of such a channel sequence typically has a fining-upward response and is essentially a textural profile beginning with relatively clean sand at the base and progressively becoming more clay-rich at the top (Fig. 2).

Marine-bar deposits have a characteristic log pattern that is opposite that of channels. In many shelf deposits, marine bars have a characteristic "cleaning"- or

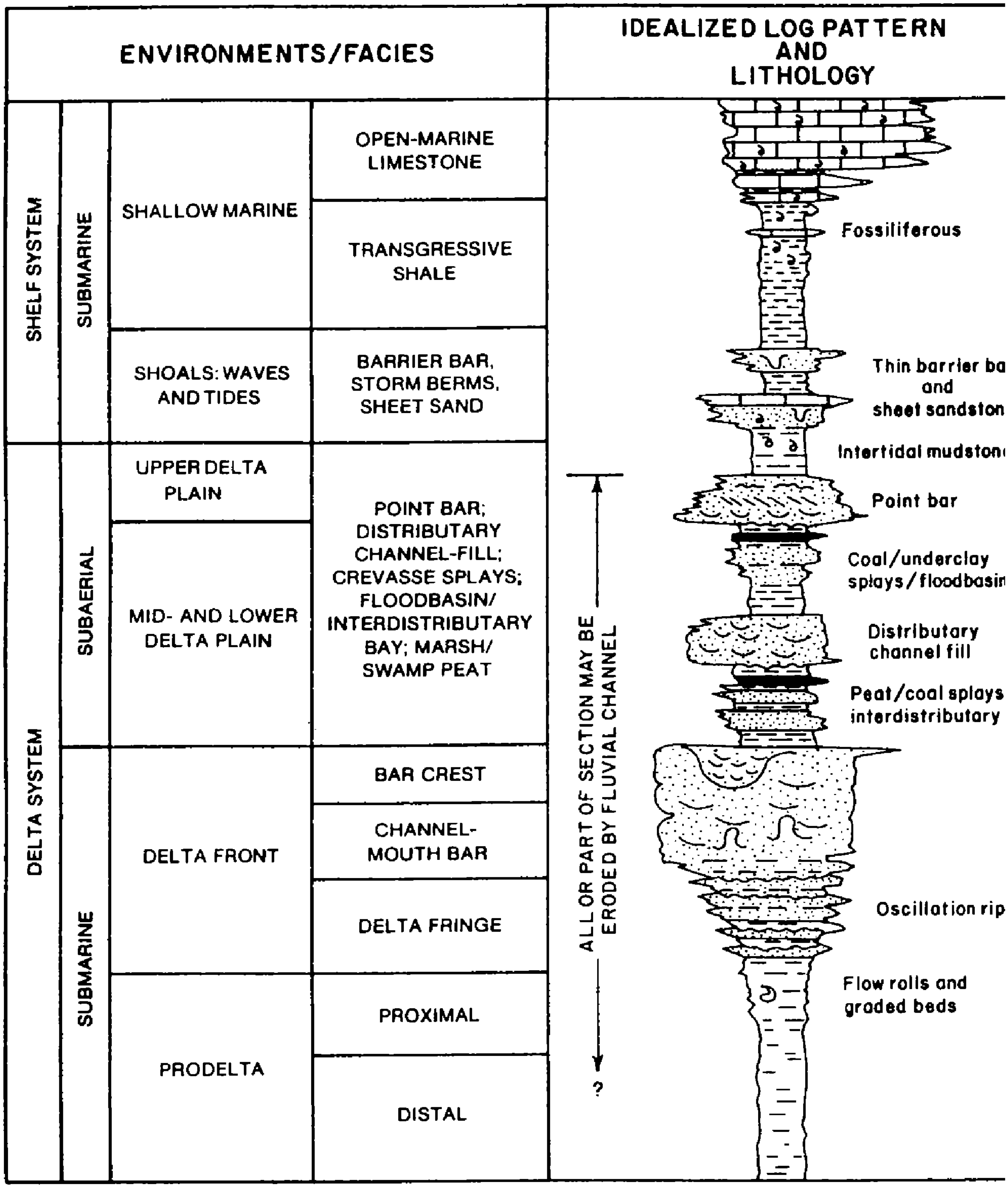

Figure 2. Idealized delta sequence showing principal depositional phases, idealized electric-log pattern, and facies description (from Brown, 1979). In this paper, "delta-fringe" refers to distributary-mouth-bar deposits that are sand-poor and occur along the edges of the delta front or in distal parts of the leading edge of the delta front. Sediments may be deposited in the bar transition or lower distributary-mouth bar. "Channel-mouth bar" and "bar crest" are upper-distributary-mouth bar in this paper; "point bar" is fluvial channel; and the lower part of the delta fringe is bar-transition. The rocks and facies shown as the shelf system (upper left) do not occur in the Hartshorne Formation.

DEPOSITIONAL PHASES		DESCRIPTION
MARINE TRANSGRESSION	SUBMARINE AGGRADATION	Commonly mixed biomicrites, fusulines near base, grades upward into algal limestone, well bedded, very fossiliferous, persistent, grades downdip into shelf-wide limestones, grades updip into brackish shales and littoral sandstones.
		Shale becomes more calcareous and fossiliferous upward, assemblage becomes less restricted, highly burrowed. In northern and eastern Mid-Continent, phosphatic black shale common at base.
DELTA DESTRUCTION		Local barrier-bar sandstone: thin, coarsening upward, commonly fringe abandoned delta. Sheet sandstone: widespread, coarsening upward, burrowed, oscillation ripples on top. Storm berm: local, shelly bars composed of broken shells. Intertidal mudstone: laminated, red/olive.
DELTA CONSTRUCTION	SUBAERIAL AGGRADATION	Point-bar sandstone: fining upward from conglomerate lag to silty levees, upward change from large trough-filled crossbeds to tabular crossbeds and uppermost ripple crossbeds. Distributary channel-fill sandstone: fine- to medium-grained, trough-filled crossbeds, local clay, clast conglomerate, abundant fossil wood. Crevasse splay sandstone: coarsening upward, trough and ripple crossbeds, commonly burrowed at top. Floodbasin/interdistributary mudstone: burrowed, marine fossils, grade updip to non-marine, silty near splays. Coal/peat: rooted, overlie underclay (soil).
	PROGRADATION	Well-sorted, fine- to medium-grained sandstone, plane beds (high flow regime) common, channel erosion increases updip, distal channel fill plane-bedded, some contemporaneous tensional faults.
		Fine- to medium-grained sandstone, trough-filled crossbeds common, commonly contorted bedding, local shale or sand diapirs in elongate deltas.
		Fine-grained sandstone and interbedded siltstone and shale, well-bedded, transport ripples, oscillation ripples at top of beds, growth faults in lobate deltas, some sole marks and contorted beds at base.
		Silty shale and sandstone, graded beds, flow rolls, slump structures common, concentrated plant debris.
		Laminated shale and siltstone, plant debris, ferruginous nodules, generally unfossiliferous near channel mouth, grades downdip into marine shale/limestone, grades along strike into embayment mudstones.

coarsening-upward textural profile (Figs. 1,2). Although there is a variety of marine-bar environments—e.g., detached shelf bars, distributary-mouth bars, and barrier islands—the depositional processes forming them generally are similar. Therefore, these types of deposits commonly exhibit similar textural and gamma-ray profiles. In typical marine-bar deposits such as those mentioned above, the lower part of the bar complex (bar-transition facies) is composed of interbedded mud, silt, and very fine grained sand. The thickness of the bar-transition facies can be highly variable. Higher in the marine-bar sequence, individual sand beds become thicker, and the amount of interbedded mud and silt decreases. The upper-bar facies contains little interstitial clay or interbedded mud, and the sand-grain size typically is greater than that lower in the sequence. Therefore, the textural profile coarsens or "cleans" upward (Figs. 1,2). The type of marine bar can also be interpreted on the basis of the nature of the overlying sediments. A coarsening-upward clastic sequence may be interpreted as a distributary-mouth bar (of the delta front) if delta-plain deposits (channel sand, coal, interdistributary bay-fill sediments, etc.) occur directly above the marine-bar sequence. In this case, the marine-bar to delta-plain sequence represents delta progradation.

Profiles of Deltas

Brown's (1979) description of deltaic facies and their electric-log patterns is accepted widely (Figs. 1,2). Gamma-ray (and commonly, resistivity) profiles of fluvial channels of the upper delta plain show a sharp basal contact and an upward-fining textural profile. Sequences containing bay-fill shale and crevasse-splay sand stone of the delta plain are characterized by a highly irregular gamma-ray profile, whereas distributary channels typically have abrupt basal and upper contacts. Distributary-mouth bars of the delta front typically have a coarsening- or "cleaning"-upward profile. The lower part of Brown's (1979) delta-fringe facies is termed *bar transition* in this paper, because it occurs stratigraphically between marine shale of the prodelta (characterized by relatively high gamma-ray values and flat profile) and sandstone of the distributary-mouth bar (which has a coarsening-upward profile). Most deltaic facies and log patterns described by Brown (1979) occur in the Hartshorne Formation, and most of the outcrops, surface gamma-ray profiles, and well logs of the Hartshorne can be interpreted by using Brown's (1979) model. Additional interpretations of the surface gamma-ray and wireline-log profiles are given below.

Current Study

Instrumentation and Gamma-Ray-Measuring Technique

For this project, we used a Scintrex GRS-500 gamma-ray spectrometer/scintillometer. This instrument was purchased by the Oklahoma Geological Survey for about $5,000, and all field measurements and graphing were completed by the authors. The GRS-500 utilizes two time constants (sampling rates), 1 second and 10 second. For better statistical results, we used a 10-second time constant, measuring total gamma radiation (uranium plus thorium plus potassium) above 400 keV. Readings are recorded from an analog display in a field notebook.

The procedure we used to measure the gamma-ray intensity of outcrop strata is easy. First, we made sure the batteries were fresh and adjusted the instrument to the proper spectral and time-constant settings. We then placed the instrument against the outcrop where there were no significant overhangs or other rock protrusions that would partially surround the instrument (such as in a small gully or rock cavity). This would cause gamma-ray values to be enhanced (or attenuated). Covered intervals were avoided. In relatively uniform strata (bar-transition and marine-shale sequences), we took readings 2 ft apart stratigraphically. Where rock types varied, such as interbedded sandstone and shale sequences, readings were taken every foot. We took five readings per station and recorded all stations on previously measured sections.

In the office, we entered the five readings per station into an MS Excel spreadsheet where they were numerically averaged. Using a scatter plot, we graphed the average gamma-ray values, adjusting the vertical scale to fit the measured sections. All gamma-ray readings are in counts per second (CPS).

Study Sites

Oklahoma Geological Survey Guidebook 31 (Suneson, 1998) includes 20 measured sections of the Hartshorne Formation in the Arkoma basin. Of these, 10 were visited on two field trips in November 1998. We measured the surface gamma-ray intensities and constructed gamma-ray profiles of six of the 10 sections that were visited (Fig. 3). The six sites were selected because they are accessible and well exposed, and the rocks are representative of all the deltaic environments of deposition observed in the Hartshorne Formation. In addition, five sites are near gas wells that have logs through the Hartshorne Formation.

Surface gamma-ray profiles are similar in appearance to wireline logs from nearby wells, except that the intensity of radiation is much less. This is due to the relatively small surface area of the sampled interval on the surface compared to that in a wellbore. In a wellbore, rocks completely surround the gamma-ray tool, resulting in a much higher gamma-ray count. Surface measurements ranged from

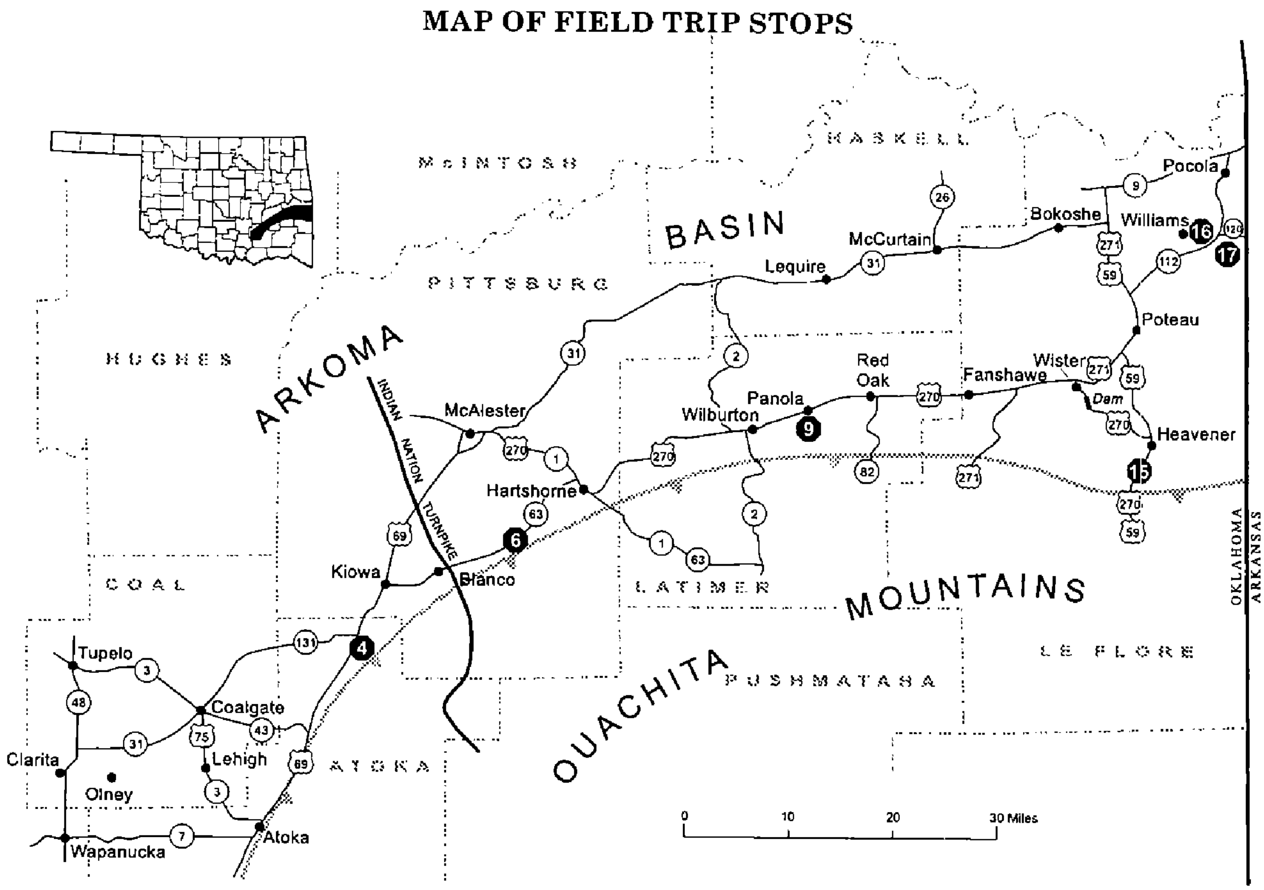

Figure 3. Map showing location of measured sections for which surface gamma-ray readings and profiles were made. Modified from Suneson (1998).

about 15 to 65 CPS, although sandstone in outcrops not profiled had readings as low as 8 CPS. Correlation of the surface gamma-ray profiles with outcrops indicates that a reading of about 40 CPS is that of the transition between mostly sandstone and mostly shale; higher values generally represent shale-dominated intervals, and lower values represent increasingly cleaner sandstones. The following is a list of stops (Fig. 3; stop numbers from Suneson, 1998) where we measured the radiation intensity of the outcrop and constructed gamma-ray profiles:

- Stop 4: Reynolds Lake measured section, S½NW¼ sec. 10, T. 2 N., R. 13 E.
- Stop 6: Gardner Creek measured section, E½E½ sec. 26, and SW¼NW¼ sec. 25, T. 4 N., R. 15 E.
- Stop 9: Panola measured section, W½E½ sec. 8, T. 5 N., R. 20 E.
- Stop 15: Heavener road cut measured section, SE¼NW¼ sec. 36, T. 5 N., R. 25 E.
- Stop 16: Williams measured section, SW¼SW¼ sec. 12, and SE¼SE¼ sec. 11, T. 8 N., R. 26 E.
- Stop 17: Green Country Stone Quarry measured section, NE¼NE¼ sec. 9 and NW¼NW¼ sec. 10, T. 8 N., R. 27 E.

Presentation of Data

Stop 4, Reynolds Lake Section (Fig. 4)

Just east of Reynolds Lake, the Hartshorne Formation is well exposed from near the top of the formation to near the base. Most of the strata in the upper half of the measured section (zones 12 to 17, Fig. 4) consist of thin-bedded, very fine grained sandstone interstratified with siltstone and shale. This sequence is interpreted as a marine delta-fringe deposit, and surface gamma-ray values are generally between 33 and 40 CPS. One thin interval at about 190–193 ft has a very low reading of about 20 CPS and has the cleanest sandstone in the upper part of the section. Most likely, the interbedded sandstone and shale were deposited in a bar-transition or possibly a lower-distributary-mouth-bar environment along the edge of the delta (fringe) rather than the active delta front. The intermediate gamma-ray values and small, low-amplitude "spikes" best characterize the transition zone or lower-distributary-mouth-bar facies in this section. Higher gamma-ray readings above 40 CPS in units 11 and 17 occur where the rock type is predominantly marine shale.

Two sandstone sequences (units 1 and 3–5, Fig. 4) in the lower part of the Reynolds Lake section have a moderately well-defined coarsening-upward gamma-ray profile, although this textural variation is not as evident in outcrop. Gamma-ray values of about 17–25 CPS are interpreted as clean to very clean sandstone. The two sandstone units are separated by a covered interval (unit 2, Fig. 4), consisting most likely of shale and siltstone. We believe that the gamma-ray readings in the covered intervals are unreliable because of the amount of cover but probably closely follow a shale baseline of about 40 CPS. In part because of the coarsening-upward gamma-ray profile and the interbedded relationship with probable marine deposits, we interpret the sandstone in units 1 and 3–5 as marine bars reworked by storm-wave processes. However, the amount of cover in the lower part of the measured section precludes a more definitive interpretation.

The surface gamma-ray profile for certain strata at Reynolds Lake is similar to the gamma-ray log of the Sunset International No. 1 Bennett well (Fig. 5), located about 2.5 mi northwest of the measured section. The relatively flat part of the sur-

STOP 4
REYNOLDS LAKE MEASURED SECTION
S/2 NW/4 sec. 10, T.2N., R.13E.

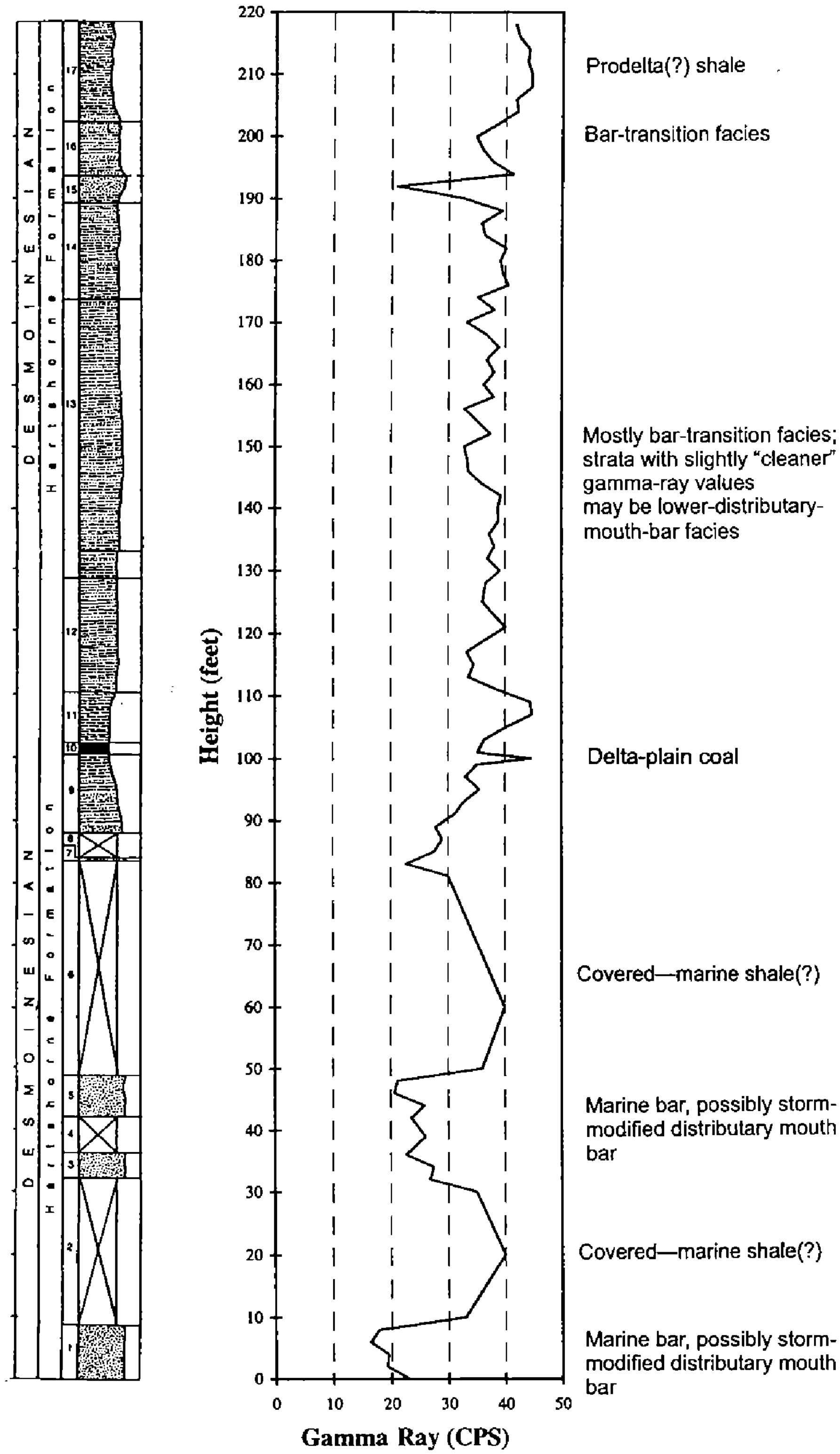

Figure 4. Columnar section and surface gamma-ray profile of part of the Hartshorne Formation exposed at Stop 4 (Reynolds Lake section). Columnar section from Suneson (1998, fig. 19).

face gamma-ray profile (Fig. 4) above the Lower Hartshorne coal (between about 110 and 190 ft) has gamma-ray values generally between 33 and 40 CPS. The rocks in this interval are very fine grained sandstone, siltstone, and shale. The same type

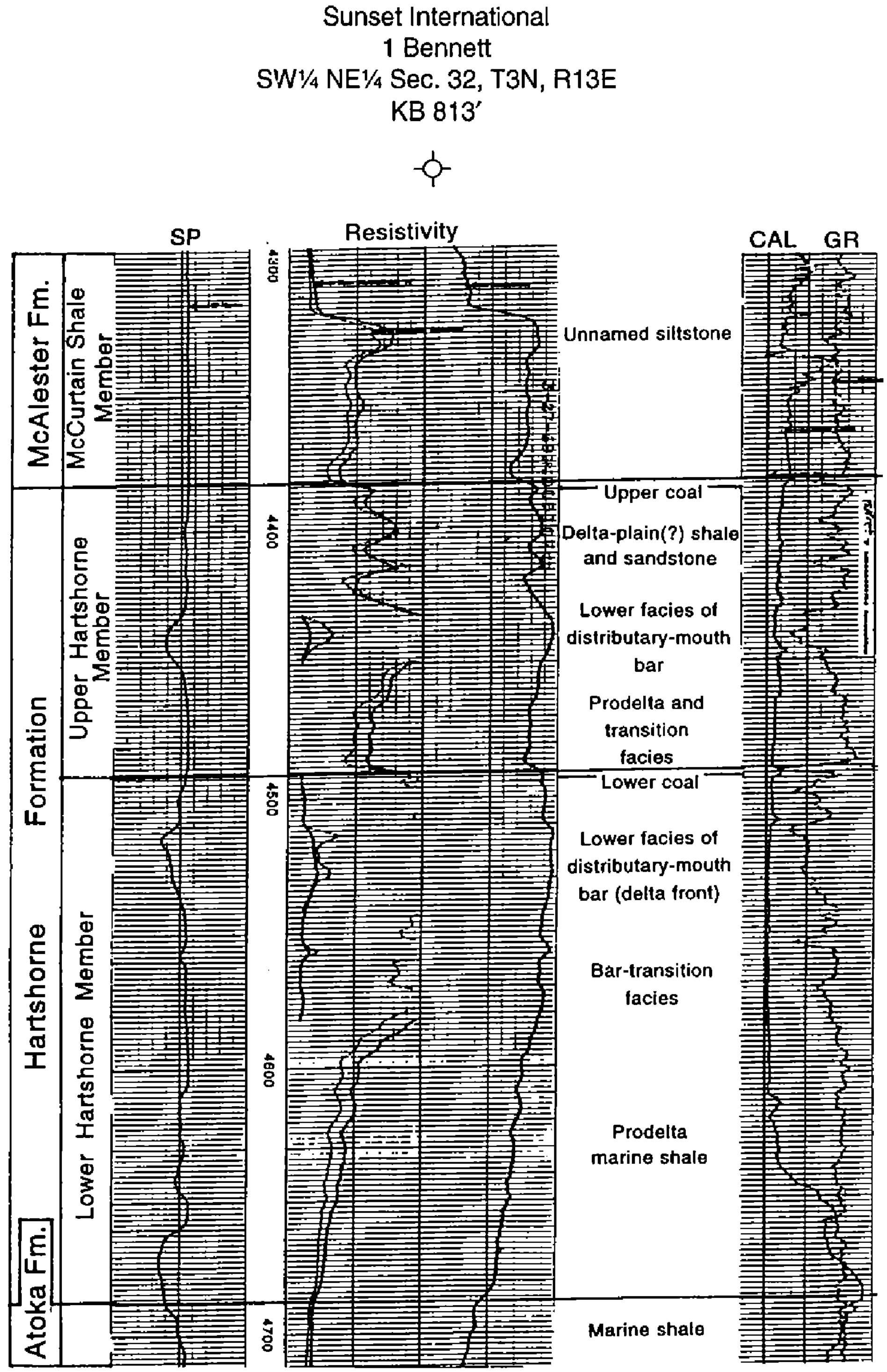

Figure 5. Part of wireline log from the Sunset International No. 1 Bennett well, drilled about 2.5 mi northwest of the Reynolds Lake section. The log signature of most of the Hartshorne Formation is typical of bar-transition and lower-distributary-mouth-bar strata. *SP* = spontaneous potential; *CAL* = caliper; *GR* = gamma ray. From Suneson (1998, fig. 21).

of gamma-ray profile occurs in the well log, particularly in the Lower Hartshorne Member between 4,580 and 4,530 ft; therefore, this interval probably contains the same rock types as those in the measured section. However, the resistivity recorded in the Bennett well throughout this interval is relatively high (mostly above 50 ohm-m), and without the gamma-ray log, this resistivity profile might be mistaken for a thick, continuous sandstone section such as that directly above it at 4,530–4,510 ft. This 20-ft section has lower gamma-ray values, which are evidence that the sandstone has little interstitial clay and few shale partings and is probably cleaner and a better reservoir than the 4,580–4,530-ft interval. Other log characteristics that support this interpretation include higher resistivity (above 100 ohm-m) and a significant spontaneous-potential (SP) deflection. The same type of log response occurs in the Upper Hartshorne Member between 4,450 and 4,430 ft, which is evidence for a relatively clean sandstone.

On the gamma-ray and resistivity logs from the Bennett well (Fig. 5), the distinct coarsening-upward sequences in the Upper and Lower Hartshorne Members (4,480–4,430 ft and 4,650–4,510 ft) are evidence for a transition from prodelta or marine shale to bar transition to distributary-mouth bar. In the surface-measured section (Fig. 4), this progression of marine facies is not as clear, although in the Upper Member (above unit 10), the cleanest sandstone occurs high in the section (unit 15, Fig. 4). The predominance of interbedded silty shale and very fine grained sandstone in the Upper Hartshorne Member at Reynolds Lake is evidence that these strata were deposited in distal parts of the delta front (or in delta-fringe areas) in comparison to deposits near the Bennett well, which were probably laid down in the active (proximal) delta front. The differences in the gamma-ray profiles support this interpretation.

Stop 6, Gardner Creek Section (Fig. 6)

As interpreted from sedimentary structures observed in the outcrop, the Lower Hartshorne Member at Gardner Creek is a distributary-mouth-bar sequence overlying the Atoka Formation. In the measured section, the base of the Hartshorne Formation is placed at the top of unit 1 at about 30 ft (Fig. 6). Below this horizon, gamma-ray values are >50 CPS, and the strata are interpreted to be marine shale and siltstone (unit 1, Fig. 6) in the uppermost part of the Atoka Formation. In the lower part of the Hartshorne Formation, units 2 and 3 consist of shale, siltstone, and sandstone that show an overall coarsening-upward gamma-ray profile. The gamma radiation decreases from about 42 CPS at the top of unit 2 to just over 20 CPS at the top of unit 3. From bottom to top, this sequence represents prodelta, bar-transition, and lower- to (minor) upper-distributary-mouth-bar sediments. The two thin sandstones with relatively low gamma-ray values (~33 CPS) just above 30 ft may represent coarser sediments reworked by storm events in an otherwise fine-grained sequence.

The gamma-ray profile of units 4 and 5 (Fig. 6) also shows an overall coarsening-upward sequence. Unit 4 is a relatively monotonous interval consisting of siltstone, sandstone, and minor shale with gamma-ray values mostly between about 35 and 40 CPS. This is probably a progradational sequence consisting of bar-transition and lower-distributary-mouth-bar strata similar to those in the Upper Hartshorne Member at Reynolds Lake. These strata "clean" upward to unit 5, which consists of two intervals, each about 10 ft thick, of 17–25-CPS sandstone. These values are

STOP 6

GARDNER CREEK SECTION

E/2 E/2 sec. 26, and SW/4 NW/4 sec. 25, T.4N., R.15E.

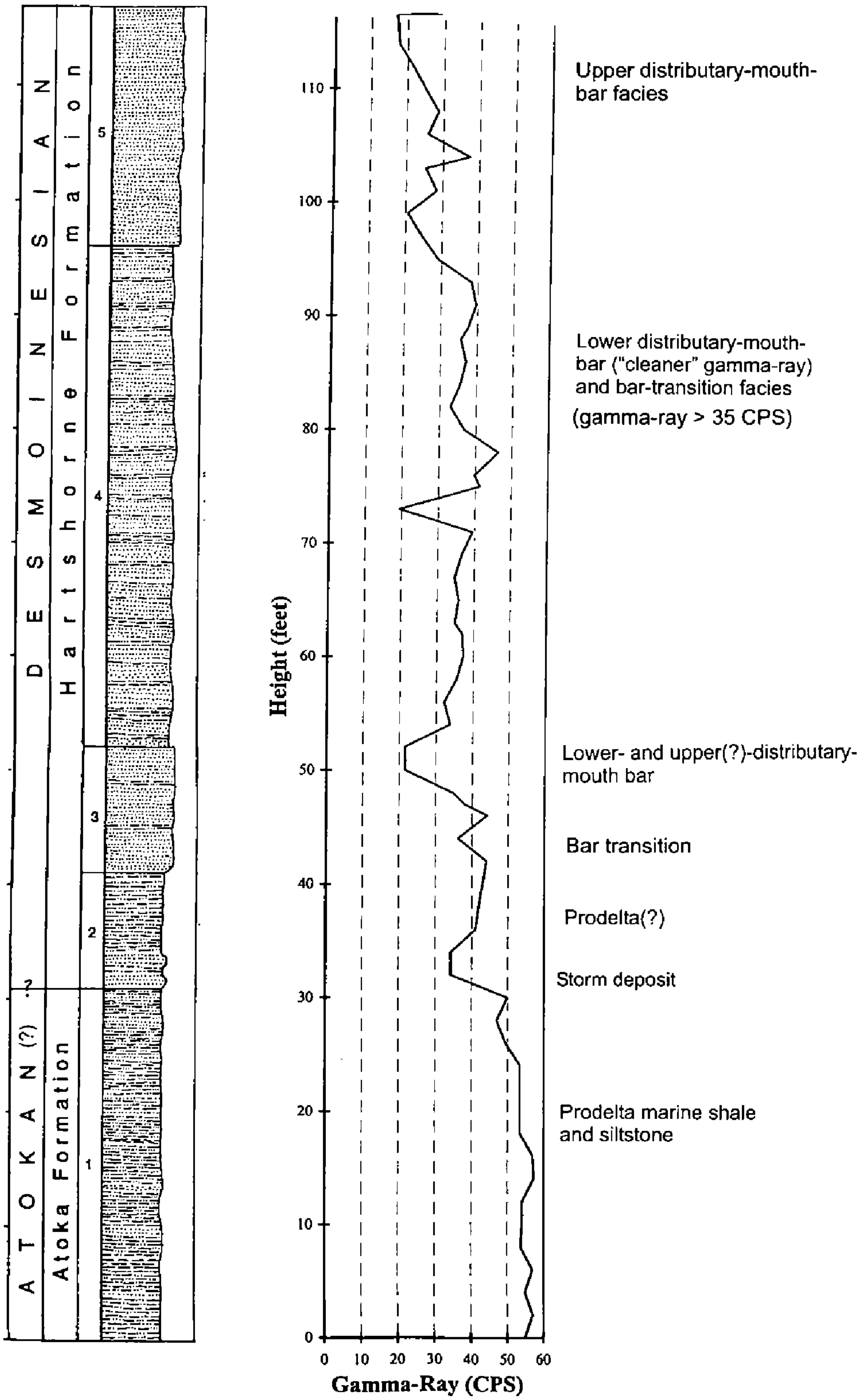

Figure 6. Columnar section and gamma-ray profile of part of the Hartshorne Formation and upper Atoka Formation exposed at Stop 6 (Gardner Creek section). Columnar section from Suneson (1998, fig. 27).

some of the lowest of any sandstone in this study and indicate very little interstitial clay or interbedded shale. This interpretation is supported by field observations that show the sandstone to be composed almost entirely of quartz. Sedimentary features include large-scale, high-angle cross-bedding typical of the upper-distributary-mouth-bar facies (equivalent to an upper-shoreface environment). These types of sandstones constitute the primary marine reservoir in subsurface exploration (Andrews and others, 1998, p. 22).

Figure 7 is part of the well log from the Mustang Production No. 1 Browne well, located about 3 mi northwest of the Gardner Creek section. As interpreted from this well log, the Lower Hartshorne Member consists of about 160 ft (5,160–5,000 ft) of bar-transition and prodelta sediments overlain by three coarsening-upward marine-bar sequences at 5,000–4,960, 4,950–4,872, and 4,870–4,780 ft. The clean, reservoir-quality sandstone at 4,800–4,780 ft in the top part of the highest bar sequence probably correlates with the clean sandstone in unit 5 on the measured section (Fig. 6). The bottom part of the upper-bar sequence and the middle-bar sequence in the Browne well probably correlate with unit 4 at the surface. These intervals in the well log and measured section have low to intermediate gamma-ray values, which is evidence for some interbedded shale. Units 2 and 3 (Fig. 6) appear to correlate with the lower-bar sequence in the well (5,000–4,960 ft). If our correlation is correct, the Hartshorne–Atoka contact on the well log (5,160 ft) is about 180 ft below where it is identified on the measured section. This is evidence that the Hartshorne delta-front sequence thickens moderately to the northwest in a manner consistent with the development of individual delta lobes. The relatively consistent and high gamma-ray values for the Atoka Formation in the Browne well (below 5,160 ft) are consistent with the high gamma-ray values (>50 CPS) recorded for the Atoka at the surface (unit 1).

Stop 9, Panola Section (Fig. 8)

The Panola measured section is the only locality in the Arkoma basin where most of the Hartshorne Formation, the Lower and Upper Hartshorne coals, and the upper and lower contacts of the Hartshorne Formation are exposed. Based on field observations, the Hartshorne Formation at Panola consists of marine sandstone, siltstone, and shale deposited in distributary-mouth-bar and bar-transition environments, and delta-plain deposits consisting of bay-fill shale and coal (no splay sandstone was identified).

Three coarsening-upward sandstone sequences are interpreted from the surface gamma-ray profile (Fig. 8) at 45–85, 95–136, and 175–209 ft. From outcrop observations, all three sequences have a coarsening-upward textural profile, beginning with shale and progressing upward into interbedded sandstone and shale, and finally into thick-bedded sandstone at the top of the bar sequences. The lowest sequence is gradational; the upper two are relatively abrupt. These textural relationships are clearly shown on the surface gamma-ray profiles (Fig. 8). The typical gamma-ray response for the three coarsening-upward sequences varies from >40 CPS in the underlying shale to about 30 CPS in the thicker-bedded sandstone on top of the bar sequences.

The interpreted depositional environments of strata in the Panola section are based on field observations and gamma-ray profiles. The lowest coarsening-upward sequence represents, from bottom to top, prodelta shale (top of unit 1, Fig. 8,

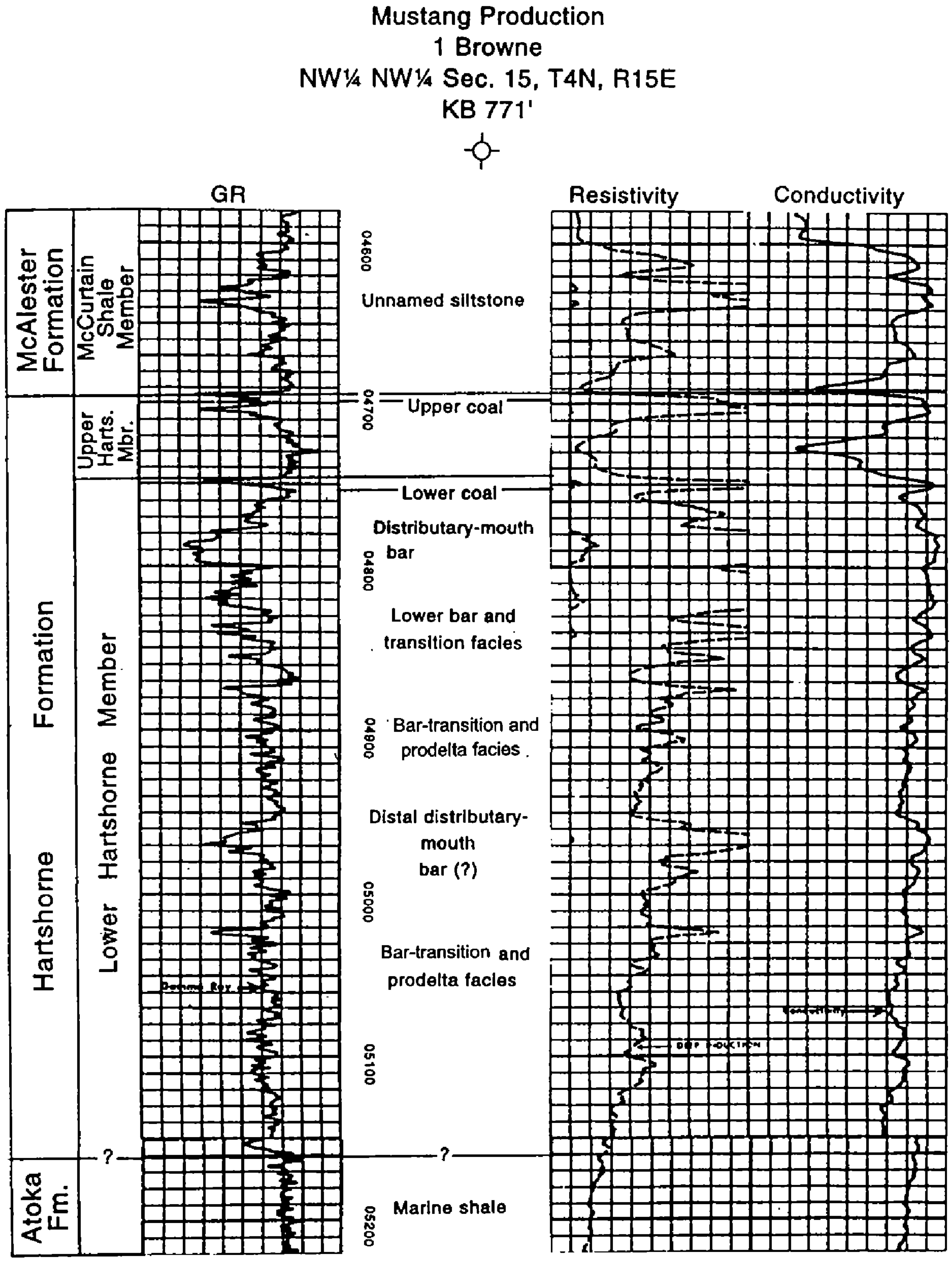

Figure 7. Part of wireline log from the Mustang Production No. 1 Browne well, showing the Hartshorne Formation. The log exhibits a 20-ft-thick upper-distributary-mouth-bar sandstone at about 4,780–4,800 ft, overlying a thick bar-transition and lower-distributary-mouth-bar facies within the Hartshorne Formation. Strata below 4,980 ft could be included in the Atoka Formation, as shown in Figure 6. This would more closely match that observed in outcrop. *GR* = gamma ray. From Suneson (1998, fig. 29).

STOP 9
PANOLA MEASURED SECTION
W/2 E/2 sec. 8, T.5N., R.20E.

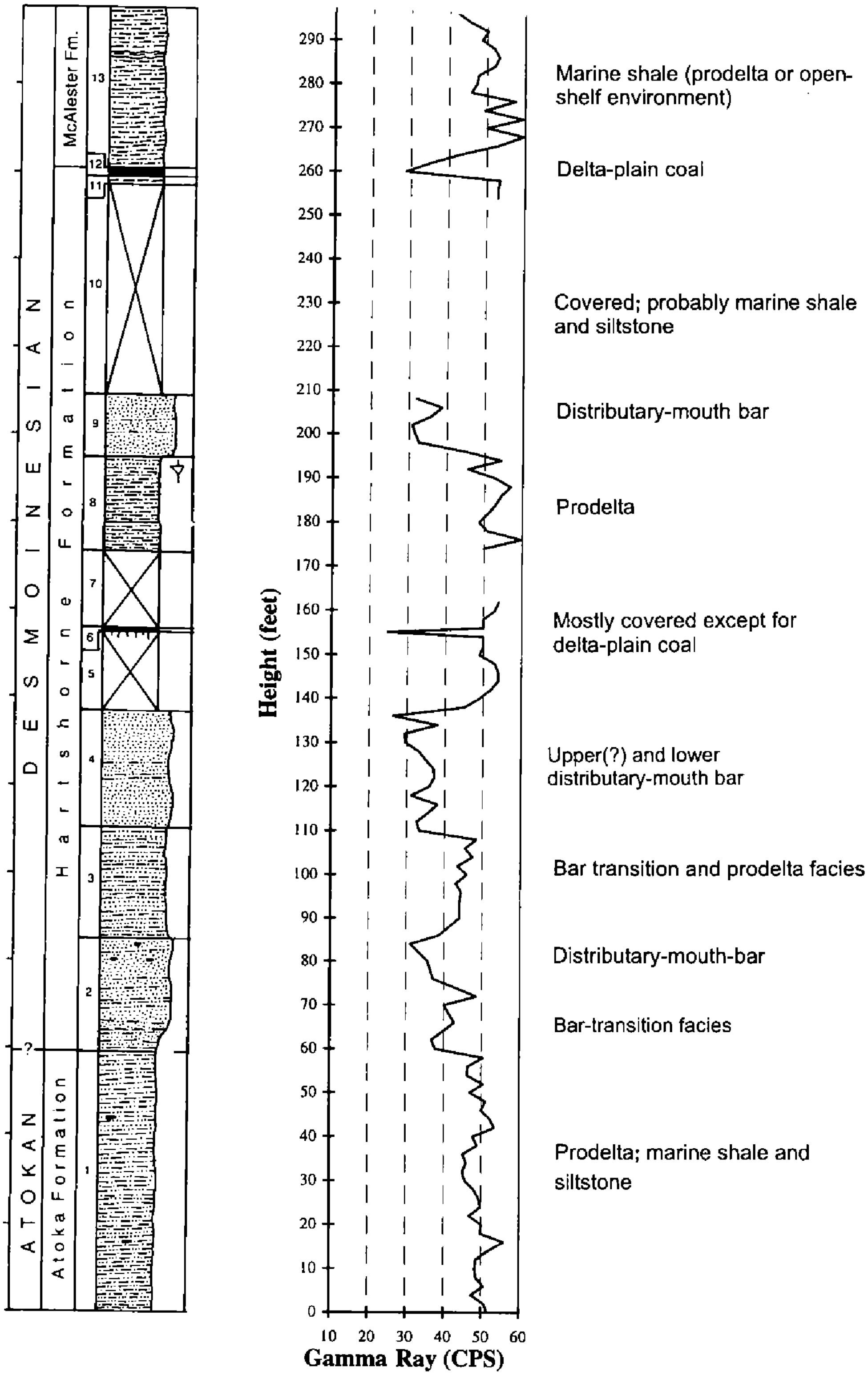

Figure 8. Columnar section and gamma-ray profile of the Hartshorne Formation, upper part of the Atoka Formation, and lower part of the McCurtain Shale Member of the McAlester Formation exposed at Stop 9 (Panola section). Columnar section from Suneson (1998, fig. 37).

gamma-ray values >45 CPS), bar-transition with minor distributary-mouth-bar(?) strata (lower part of unit 2, gamma-ray values about 36–40 CPS), and lower-distributary-mouth-bar facies (top part of unit 2, gamma-ray values about 30–36 CPS). The middle sequence consists of prodelta and bar-transition facies (unit 3, gamma-ray values about 43–48 CPS), and lower- and upper(?)-distributary-mouth-bar strata (unit 4, gamma-ray values about 26–36 CPS).

The upper coarsening-upward sequence (above the Lower Hartshorne coal—unit 6) is more difficult to interpret because of the abrupt contact, both in outcrop and on the gamma-ray profile, between units 8 and 9. Unit 8 is probably prodelta marine shale, which exhibits some of the highest gamma-ray values in the measured section (50–60 CPS), and unit 9 is probably another thin distributary-mouth-bar deposit with gamma-ray values slightly more than 30 CPS. The presence of high-angle cross-stratification in the sandstone is evidence that the bar may have been reworked by storm waves.

Figure 9 is a log from the Tenneco No. 1-29 Pierce well, which was drilled about 3.25 mi north of the measured section. As interpreted from gamma-ray and resistivity logs, Hartshorne strata in the Pierce well are more shaly than at the surface-measured section, although the same sequence of lithofacies is present. That the upper and lower contacts of the Hartshorne on the measured section and in the well are correctly identified supports the observation that the Hartshorne section in the Pierce well is considerably thinner than at the Panola section (~132 versus ~200 ft). This is evidence that strata at the surface locality are more proximal to the Hartshorne delta than those at the subsurface locality.

The Upper Hartshorne Member (above the Lower Hartshorne coal) in the Pierce well (Fig. 9) consists predominantly of shale, based on interpretation of the gamma-ray and resistivity logs. The shale interval (3,844–3,822 ft) with high gamma-ray values is correlative with a similar (but thicker) interval at the surface (unit 8, Fig. 8); both probably are prodelta marine shales. This marine shale is, in turn, overlain by a "sandy" zone in the well (3,808–3,822 ft) that may correlate with surface sandstone unit 9. The vertical transition from shale to "sandy" strata in the Pierce well is best represented by the gradual increase in resistivity that is evidence for a coarsening-upward (progradational) sequence. The moderately high gamma-ray response of the "sandy" interval in the Pierce well indicates the presence of a relatively large amount of shale or interstitial clay rather than sandstone. This may be due to sediment bypass in "fringe" areas of the delta that are more closely associated with coal development such as that directly above the sandy zone (3,802–3,798 ft). A similar general stratigraphic sequence and gamma-ray profile characterize the measured section (Fig. 8); therefore, a similar depositional environment is probable: prodelta shale grading upward into delta-fringe or lower-delta-front strata, overlain by delta-plain coal.

The Lower Hartshorne Member in the Pierce well (Fig. 9) is also considerably more shaly than the equivalent strata in the Panola measured section, although the overall sequence, as interpreted from gamma-ray and resistivity logs, is similar. Two sandy zones in the Lower Member are present in the Pierce well; one is at the base, and another near the top just below the Lower Hartshorne coal. As can be seen best on the resistivity log, the upper sandy interval has a distinct "cleaning"-upward textural profile from 3,894 to 3,854 ft, as evidenced by the upward increase in resistivity. This log response is similar to the gamma-ray profile of sandstone in unit 4 of the measured section (Fig. 8). If this correlation is correct, the gamma-ray

Tenneco
1–29 Pierce
S½ NW¼ Sec. 29, T6N, R20E
KB 1156′

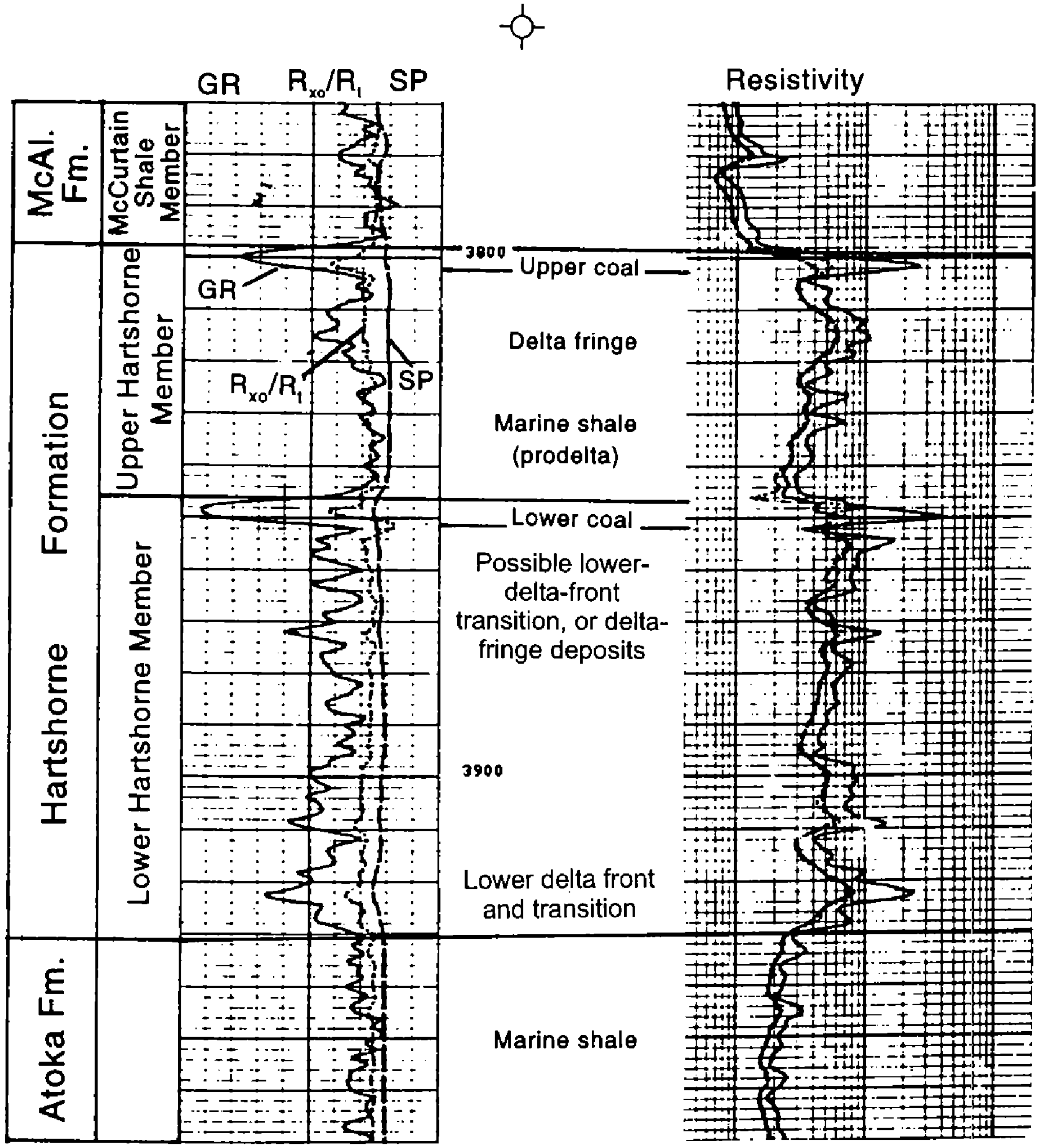

Figure 9. Part of wireline log from the Tenneco No. 1-29 Pierce well, showing the Hartshorne Formation. Similarities between the well log and measured section appear in both members of the Hartshorne Formation. In the Upper Hartshorne Member, a sandstone or sandy zone overlies a marine shale with high gamma-ray values. In the Lower Hartshorne Member, two sandy zones occur: one near the base and the other near the top. The upper sandy zone in the Lower Member has a "cleaning"-upward profile in the log and the measured section. The lower zone in the well log and surface section exhibits a gamma-ray profile that is not distinct with regard to facies recognition. *GR* = gamma ray; R_{xo} = resistivity of flushed zone; R_t = resistivity of uninvaded zone (true or deep resistivity); *SP* = spontaneous potential. From Suneson (1998, fig. 39).

profiles are evidence that the sandstone of unit 4 is considerably cleaner than the equivalent interval in the well. This supports the interpretation that the Hartshorne Formation in the Pierce well is less proximal and contains less clean sandstone than the Hartshorne at the Panola measured section.

The lower sandy interval in the Pierce well (3,930–3,898 ft) has two sandy zones that correlate with those identified from the gamma-ray profile of unit 2 in the Panola measured section (Fig. 8). However, the depositional environment is difficult to interpret because the gamma-ray profile in the well log generally lacks a distinct textural trend. The absence of a pronounced "clean" sandstone in the profile is evidence that this zone probably consists of interstratified siltstone, shale, and very fine grained sandstone and contains little moderately clean sandstone such as the sandstone in unit 2. Because the lower sandy zone directly overlies marine shale, it probably was deposited in a marine delta-fringe environment rather than an active delta front, which better characterizes unit 2 in the measured section.

Stop 15, Heavener Road Cut Section (Fig. 10)

Suneson (1998, p. 58) described the Hartshorne Formation at the Heavener road cut as follows: "This outcrop of the Hartshorne Formation . . . has been visited by more geologists than all the other Hartshorne outcrops in the State combined. Although truly spectacular and an excellent example of delta-plain sediments . . . it is atypical of most exposed Hartshorne strata in the southern part of the Arkoma basin. As discussed at previous stops, most of the Hartshorne consists of delta-front sandstone, siltstone, and shale. This outcrop, perhaps more than any other in Oklahoma, probably has caused geologists to think of the Hartshorne Formation in terms of a delta model."

As interpreted from outcrop examination, the Atoka and thick Hartshorne section in the Heavener road cut is composed entirely of delta-plain sediments—i.e., marsh/swamp and bay-fill shale, coal, and crevasse-splay sandstones. The lower ~77 ft (units 1–12, Fig. 10) consists of dark-gray to black shale with numerous thin coal beds and coal laminations. Gamma-ray values in this interval are 45–55 CPS, and the profile is relatively flat, which is typical for marsh and bay-fill shale deposits. Based on the scarcity of sandstone beds in comparison to their abundance above, this interval was interpreted by Suneson (1998) and Donica (1978) as the Atoka Formation. However, the delta-plain depositional environment of these units is evidence that they may be part of the Hartshorne Formation.

The middle and upper parts of the measured section contain numerous sandstone beds, generally only a few feet thick and separated by predominantly shale intervals (Fig. 10). Most of the sandstone beds have sharp basal contacts with the underlying shale units; this is typical of splay deposits. The presence of abundant tilted *Calamites* stumps in growth position at the bases of many of the sandstone beds is also strong evidence that the crevasse-splay sands were deposited during flood events in an interdistributary-bay environment. The sandstones are separated by shaly, organic-rich bay-fill or swamp deposits. The highly irregular gamma-ray profile in the middle and upper parts of the Heavener road cut (gamma-ray values between 22 and >50 CPS) reflects these different rock types and is characteristic of a delta-plain sequence. The profile differs from that of a typical marine distributary-mouth-bar sequence, which usually shows a continuous or gradational coarsening-upward gamma-ray profile. The profile at Heavener also differs from

STOP 15
HEAVENER ROADCUT MEASURED SECTION
SE/4 NW/4 sec. T.5N., R.25E.

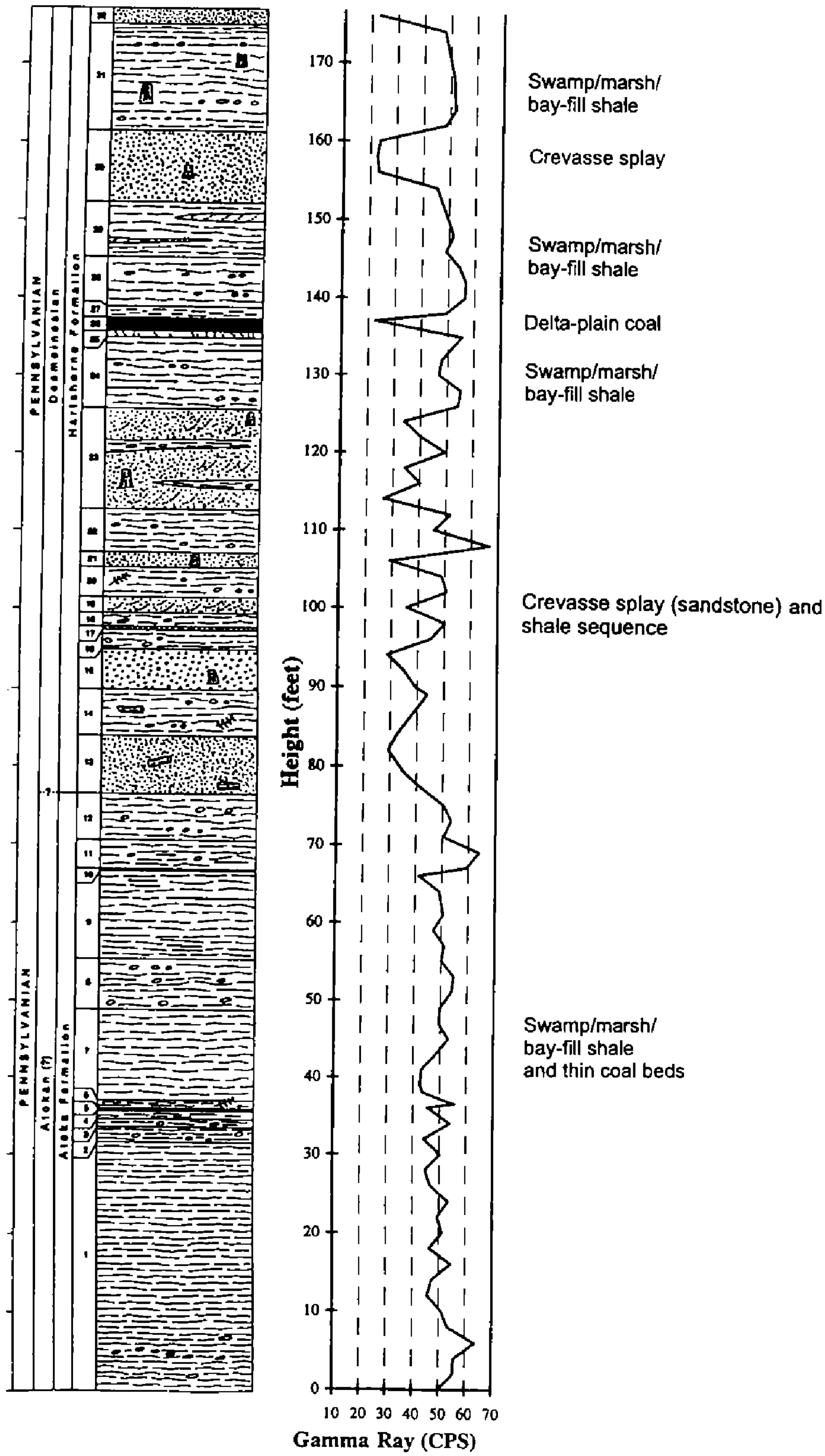

Figure 10. Columnar section and gamma-ray profile of the upper part of the Atoka Formation and the lower part of the Hartshorne Formation exposed at Stop 15 (Heavener road cut section). Columnar section from Suneson (1998, fig. 60).

that of a fluvial-channel sandstone, which is generally characterized by a gamma-ray profile having an abrupt base and a progressively "cleaning"-downward textural profile.

The Lower Hartshorne coal (unit 26, Fig. 10) exhibits low gamma-ray values, as in most surface profiles and well logs.

The Mobil No. 1 Ann Lyons well was drilled about 7 mi north-northeast of the Heavener road cut. On the basis of the gamma-ray log (Fig. 11), the rock types and depositional environments are interpreted to be similar to those of the Heavener road cut. Most of the Lower Hartshorne Member at about 1,103–1,165 ft on the log (Fig. 11) expresses a highly irregular gamma-ray profile, resembling that in units 13–23 in the measured section (Fig. 10). The sequence causing this gamma-ray profile is interpreted to be crevasse-splay sandstones interbedded with bay-fill shales. Above the splay sequence and below the Lower Hartshorne coal is a shale interval 42 ft thick in the well (Fig. 11) and ~10 ft thick in outcrop (unit 24, Fig. 10). In the well and outcrop, this shale is characterized by high gamma-ray values and a relatively flat gamma-ray profile. The stratigraphic position of this shale in the well log (above splay deposits and below coal) is evidence that it probably was deposited in a delta-plain environment. This interpretation is supported by detailed field observations of the same shale interval in the measured section.

On the well log (Fig. 11), a 20-ft-thick sandstone directly above the lower coal in the Upper Hartshorne Member is progressively overlain by shale with high gamma-ray values and a thin coal with a low gamma-ray value (Upper Hartshorne coal, 984–985 ft). This stratigraphic succession is also indicative of a deltaic environment and is generally similar to the delta-plain sediments at the outcrop. Therefore, the high-value shale in the Lyons well probably is swamp/marsh bay-fill material, and the sandstone either is a distributary channel or a proximal splay deposit. The relatively low, blocky gamma-ray values of the sandstone on the well log and the slightly fining-upward gamma-ray response support this interpretation.

Stop 16, Williams Section (Fig. 12)

The Williams measured section includes the lower part of the Hartshorne Formation and the uppermost part of the Atoka Formation. The section consists of about 90 ft of marine shale and delta-front sandstone that is relatively well exposed despite the unimpressive nature of the outcrop. As with other measured sections containing delta-front sediments, siltstone and very fine grained sandstone are abundant. Gamma-ray profiles are effective in identifying this type of lithology, as discussed below.

The surface gamma-ray profile of units 3–6 (Fig. 12) shows an overall coarsening-upward textural profile that is characteristic of a progradational distributary-mouth-bar sequence. An important aspect of this profile is that the coarsening-upward nature of the strata includes the uppermost part of the Atoka Formation and is evidence that the top of the Atoka Formation is part of the same depositional sequence as the lower part of the Hartshorne Formation. Based on the rock types and sedimentary structures observed in outcrop, the basal part of this progradational sequence (unit 3) consists of prodelta marine shale of the Atoka Formation that is progressively overlain by bar-transition (unit 4) and lower-distributary-mouth-bar sediments of the Hartshorne Formation (units 5 and 6). The contact between the Atoka and Hartshorne Formations in outcrop is marked by an abrupt transition from silty shale in the upper Atoka to thin-bedded siltstone and sand-

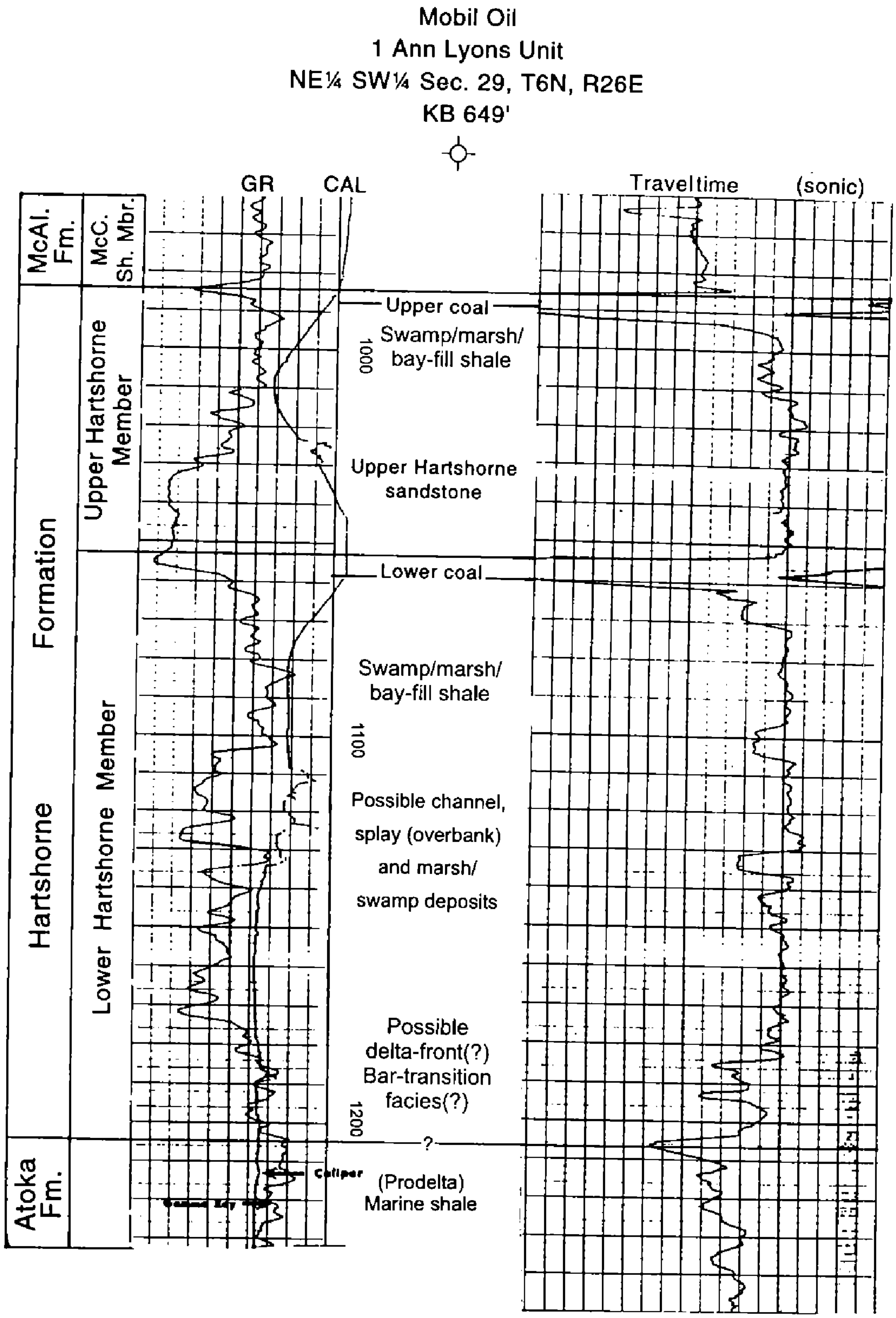

Figure 11. Part of wireline log from the Mobil No. 1 Ann Lyons well, showing the Hartshorne Formation. The gamma-ray (*GR*) profile of the upper and middle parts of the Lower Hartshorne Member is characteristic of delta-plain deposits. The lower part of the Hartshorne Formation (bar transition) and the upper part of the Atoka Formation (marine) on the log are different from those exposed at Stop 15 (Heavener road cut). *CAL* = caliper. From Suneson (1998, fig. 62).

STOP 16
WILLIAMS SECTION
SW/4 SW/4 sec. 12, T.8N., R.26E.

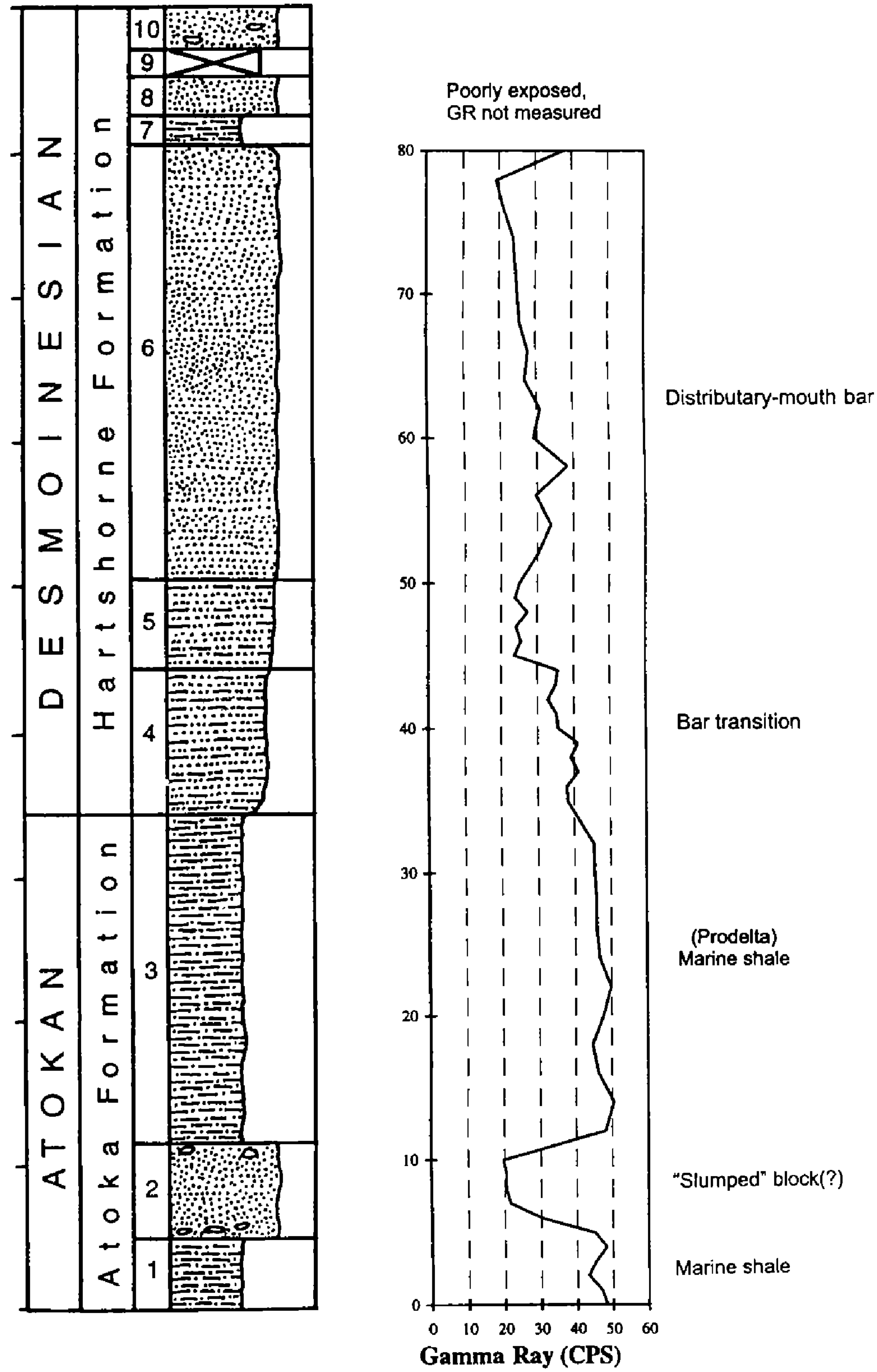

Figure 12. Columnar section and gamma-ray profile of the upper part of the Atoka Formation and the lower part of the Hartshorne Formation exposed at Stop 16 (Williams section). Columnar section from Suneson (1998, fig. 63).

stone in the basal Hartshorne. The gamma-ray response across this interval reflects the lithologic change and decreases from about 45–50 CPS in the prodelta marine-shale sequence to about 33–40 CPS in the basal Hartshorne bar-transition facies. The uppermost part of the delta-front sequence in the Hartshorne outcrop (unit 5 and top half of unit 6) contains relatively clean sandstone with very low (<25 CPS) gamma-ray values. These low values are evidence that the sandstone contains little interstitial clay or interbedded shale. Because of this and the ripple-bedded nature of the sandstone, these deposits are interpreted to be part of a lower-distributary mouth-bar sequence. The lower part of unit 6 has slightly higher gamma-ray values than unit 5 or the upper part of unit 6; the absence of interbedded shale in the outcrop is evidence that the sandstone in the lower part of unit 6 may contain more interstitial clay than the sandstone directly above and below.

The Lower Hartshorne Member in the Trigg No. 1 Basham-French well (Fig. 13), drilled about 3.5 mi south-southeast of the Williams section, has a generally similar gamma-ray profile to that of the outcrop. The wireline log of the well shows three "cleaning"-upward clastic sequences. The lowest sequence (below ~1,560 ft) probably correlates with that exposed in outcrop because only the lowest part of the Hartshorne Formation is exposed at the Williams section. The gradual "cleaning"-upward gamma-ray profile in the log characterizes bar-transition to lower-distributary-mouth-bar facies. Clean sandstones typical of an upper-distributary-mouth-bar environment are rare in the well because the gamma-ray values stay close to the shale baseline. (The maximum log response is only ~3 units to the left of that recorded in shale.) This same type of gamma-ray response occurs in the measured section (Fig. 12) through unit 4 and in the lower part of unit 6, where gamma-ray values approach those of the shaly intervals. Based on similar gamma-ray profiles, strata in the Basham-French well probably consist mostly of interbedded siltstone, very fine grained sandstone, and shale with few clean sandstone intervals.

The resistivity log of the lower sandy interval (below about 1,560 ft; Fig. 13) can be better interpreted when the similarity of the surface and subsurface gamma-ray profiles is recognized. As shown in Figure 13, the lower sandy interval that correlates with the surface section is characterized by relatively high resistivity (>50 ohm-m), which may be mistaken for good reservoir quality and moderate sandstone thickness. Using the generally similar gamma-ray profile from the measured section, most of the strata in the lower coarsening-upward sequence in the well (1,560–1,618 ft; Fig. 13) probably is shaly, with relatively little clean sandstone. This interpretation is supported by the flat bulk-density log (not shown).

Stop 17, Green Country Stone Quarry Section (Fig. 14)

The Green Country Stone Quarry measured section exposes an excellent example of a thin lower-delta-plain distributary-channel sandstone overlying delta-front distributary-mouth-bar deposits. In the measured section, the marine delta-front unit (unit 1, Fig. 14) consists mostly of moderately thick sandstone beds interstratified with thin shale beds. The gamma-ray profile across unit 1 shows a gradual "cleaning" upward, evidence that the amount of shale increases slightly downward to the base of the section. This "cleaning"-upward profile is characteristic of distributary-mouth bars. Prodelta or bar-transition deposits that would normally underlie the distributary-mouth bars are not exposed in the quarry, although the relatively high gamma-ray values in unit 1 (above 40 CPS) are normally associated with shale. The high gamma-ray values of the sandstone and interbedded

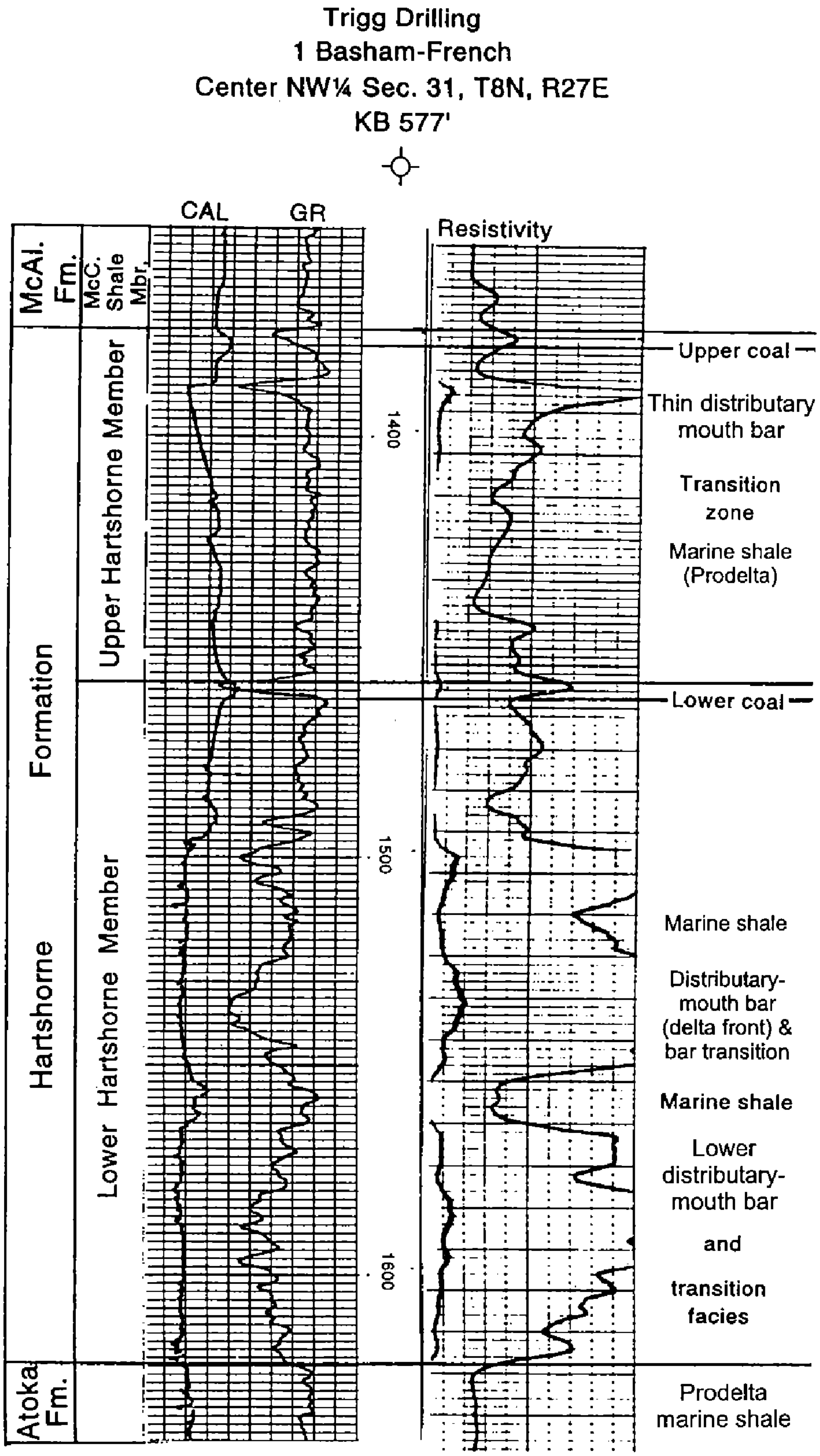

Figure 13. Part of log from the Trigg No. 1 Basham-French well, showing the Hartshorne Formation. In the Lower Hartshorne Member in the Trigg well, two coarsening-upward sandstone sequences below 1,520 ft are similar to sandstone sequences in the measured section (Fig. 12). These log signatures are characteristic of bar-transition and lower-distributary-mouth-bar deposits. *CAL* = caliper; *GR* = gamma ray. From Suneson (1998, fig. 65).

STOP 17
GREEN COUNTRY STONE QUARRY MEASURED SECTION
NE/4 NE/4 sec. 9 and NW/4 NW/4 sec. 10, T.8N., R.2E.

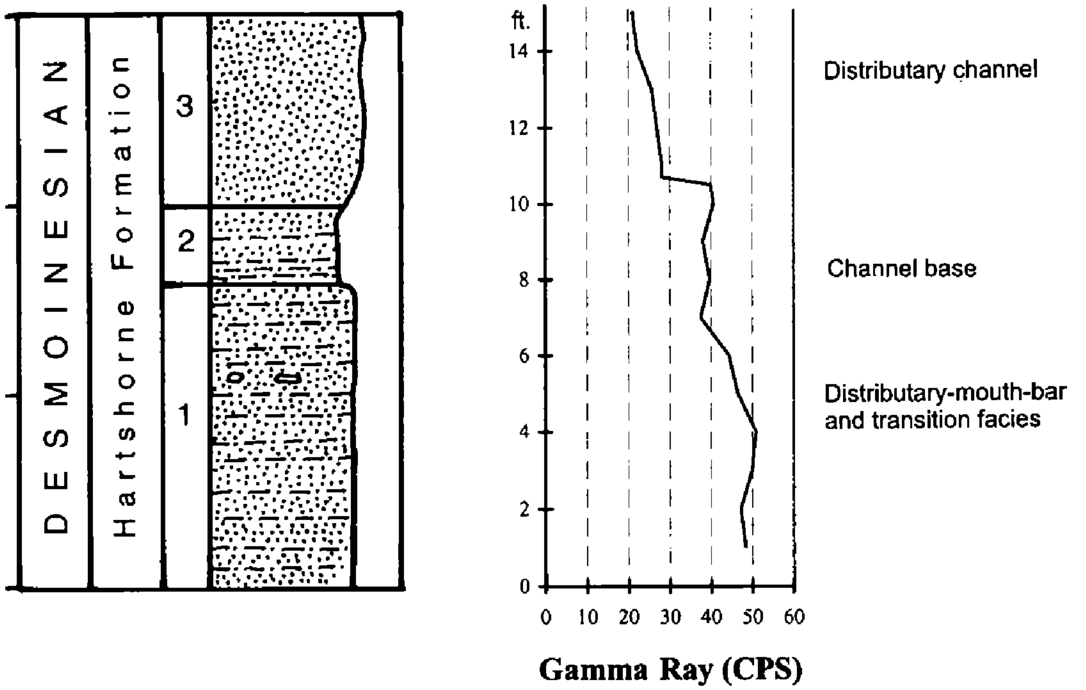

Figure 14. Columnar section and gamma-ray profile of part of the Hartshorne Formation exposed at Stop 17 (Green Country Stone Quarry section). Columnar section from Suneson (1998, fig. 67).

shale interval shown in Figure 14 are uncharacteristic of such sandy strata, for which no explanation is evident.

Where the gamma-ray profile was measured, the base of the channel complex (base of unit 2, Fig. 14) is mostly shale. The base of the channel-fill sandstone is slightly higher at the base of unit 3, and the gamma-ray profile reflects this lithologic break at an abrupt "step" in gamma-ray values (from about 40 to 28 CPS). The massive channel sandstone of unit 3 generally has very low readings of 20–28 CPS and indicates a scarcity of interstitial clay and interbedded shale. This contrasts with the shale-rich marine section (unit 1), which has gamma-ray values of 38–50 CPS.

Summary

Surface gamma-ray profiles of sandstone, siltstone, and shale sequences in the Hartshorne Formation are important for relating rock types, textural variations, and sedimentary facies observed in outcrop with gamma-ray logs of similar strata in subsurface well logs. Careful study of outcrops yields information critical for depositional environmental interpretations that is not generally available from logs—for example, character of thin beds, sedimentary structures, fossils, and nature of stratal contacts and discontinuities. However, the usefulness of outcrops is limited by incomplete or poor exposures and their limited geographic distribution. In contrast, wireline logs can record continuous data through the entire thickness of a formation, and closely spaced logs give information on geographic variability.

Gamma-ray logs, which record the natural gamma radiation given off by a sequence of exposed rocks or rocks in a wellbore, are useful for interpreting lithology, depositional environments, and reservoir quality of subsurface formations. This observation is particularly true if wireline gamma-ray logs respond similarly to gamma-ray profiles of rock sequences exposed, measured, and studied at the surface. The Hartshorne Formation in southeastern Oklahoma was deposited in several different deltaic environments, including marine, prodelta, lower- and upper-distributary-mouth bars, distributary channels, interdistributary bays, lagoons, and marshes. Most of these environments can be recognized in outcrop. Surface gamma-ray profiles of the sequences in each of the environments are distinct and compare closely with standard oil-field wireline gamma-ray logs. Recognition of the different Hartshorne lithofacies on well logs enables a better understanding of the entire Hartshorne depositional system, most of which is deeply buried. This, in turn, provides for more successful exploration and development drilling of the Hartshorne Formation in the Arkoma basin.

The same principles of gamma-ray logging and interpretations used for the Hartshorne Formation can also be applied to almost all the detrital clastic sequences in the Midcontinent. In fact, this principle formed the basis of depositional interpretations of all fluvial-dominated deltaic (FDD) oil-reservoir studies published by the Oklahoma Geological Survey in its Special Publication series.

Acknowledgments

This study was prompted by a field trip and workshop on the Hartshorne Formation. These, in turn, were outgrowths of two recent and highly successful programs conducted by the Oklahoma Geological Survey: detailed geologic mapping in the Arkoma basin and Ouachita Mountains (STATEMAP), and the FDD oil-reservoir project. The STATEMAP program in southeastern Oklahoma consisted of new geologic mapping at a scale of 1:24,000 with an emphasis on resource (gas, coal, limestone, sand and gravel) and environmental (waste disposal, abandoned coal mines) issues. Twenty-two new maps have been produced under STATEMAP and its precursor, COGEOMAP, both of which were funded by the OGS and the U.S. Geological Survey. The FDD project was designed to identify and analyze all FDD light-oil reservoirs in Oklahoma and to implement an information- and technology-transfer program to help the operators of FDD reservoirs learn how to increase oil recovery and sustain the life expectancy of existing wells. Funding from the U.S. Department of Energy's Bartlesville Project Office enabled eight plays to be studied and the results reported.

References Cited

Andrews, R. D., 1995, Fluvial-dominated deltaic (FDD) oil reservoirs in Oklahoma, *part 1 of* Andrews, R. D.; Knapp, R. M.; and Bhatti, Zahid, Fluvial-dominated deltaic (FDD) oil reservoirs in Oklahoma: the Morrow play: Oklahoma Geological Survey Special Publication 95-1, p. 1–12.

Andrews, R. D.; Cardott, B. J.; and Storm, Taylor, 1998, The Hartshorne play in southeastern Oklahoma: regional and detailed sandstone reservoir analysis and coalbed-methane resources: Oklahoma Geological Survey Special Publication 98-7, 90 p.

Brown, L. F., Jr., 1979, Deltaic sandstone facies of the Midcontinent, *in* Hyne, N. J. (ed.),

Pennsylvanian sandstones of the Midcontinent: Tulsa Geological Society Special Publication 1, p. 35–63.
Coleman, J. M.; and Prior, D. B., 1982, Deltaic environments of deposition, *in* Scholle, P. A.; and Spearing, Darwin (eds.), Sandstone depositional environments: American Association of Petroleum Geologists Memoir 31, p. 139–178.
Donica, D. B., 1978, The geology of the Hartshorne coals (Desmoinesian) in parts of the Heavener 15′ quadrangle, Le Flore County, Oklahoma: University of Oklahoma unpublished M.S. thesis, 128 p.
Hemish, L. A.; and Suneson, N. H., 1997, Stratigraphy and resources of the Krebs Group (Desmoinesian), south-central Arkoma basin, Oklahoma: Oklahoma Geological Survey Guidebook 30, 83 p.
Hendricks, T. A.; Dane, C. H.; and Knechtel, M. M., 1936, Stratigraphy of Arkansas–Oklahoma coal basin: American Association of Petroleum Geologists Bulletin, v. 20, p. 1342–1356.
Houseknecht, D. W.; Zaengle, J. F.; Steyaert, D. J.; Matteo, P. A., Jr.; and Kuhn, M. A., 1983, Facies and depositional environments of the Desmoinesian Hartshorne sandstone, Arkoma basin, *in* Houseknecht, D. W. (ed.), Tectonic–sedimentary evolution of the Arkoma basin and guidebook to deltaic facies, Hartshorne sandstone: Society of Economic Paleontologists and Mineralogists, Mid-Continent Section, Guidebook, v. 1, p. 53–82.
Houseknecht, D. W.; Kuhm, M. A.; Matteo, A. P., Jr.; Steyaert, D. J.; Zaengle, J. F.; and Iannacchione, A. T., 1984, High-constructive, tidally-influenced deltaic sedimentation in the Arkoma basin: the Desmoinesian Hartshorne sandstone, *in* Borger, J. G., II (ed.), Technical Proceedings of the 1981 American Association of Petroleum Geologists, Mid-Continent Section, regional meeting: Oklahoma City Geological Society, p. 26–41.
Howe, D., 1989, Surface gamma-ray profiling technique applied to Cretaceous Ferron Sandstone, east-central Utah [abstract]: American Association of Petroleum Geologists Bulletin, v. 73, p. 365.
Jordan, D. W.; Lowe, D. R.; Slatt, R. M.; Stone, C. G.; D'Agostino, Anthony; Scheihing, M. H.; and Gillespie, R. H., 1991, Scales of geological heterogeneity of Pennsylvanian Jackfork Group, Ouachita Mountains, Arkansas: applications to field development and exploration for deep-water sandstones: Dallas Geological Society, American Association of Petroleum Geologists annual convention, Field Trip 3, 142 p.
Scruton, P. C., 1950, The petrography and environment of deposition of the Warner, Little Cabin, and Hartshorne sandstones in northeastern Oklahoma: American Journal of Science, v. 248, p. 408–426.
Slatt, R. M.; Borer, J. M.; Horn, B. W.; Al-Siyabi, H. A.; and Pietraszek, S. R., 1995, Outcrop gamma-ray logging applied to subsurface petroleum geology: Mountain Geologist, v. 32, p. 81–94.
Suneson, N. H., 1998, Geology of the Hartshorne Formation, Arkoma basin, Oklahoma: Oklahoma Geological Survey Guidebook 31, 73 p.
Yeakel, L. S., 1966, Hartshorne Formation, *in* Le Blanc, Rufus (ed.), Paleozoic sandstones of Arkoma basin and Ouachita Mountains, northwestern Arkansas and eastern Oklahoma: Unpublished field-trip guidebook, Shell Oil Co., Houston, p. 14–24.

Oklahoma Earthquakes, 1998

James E. Lawson, Jr.,[1] *and Kenneth V. Luza*[2]

Introduction

More than 930,000 earthquakes occur throughout the world each year (Tarbuck and Lutgens, 1990). Approximately 95% of these earthquakes have a magnitude of <2.5 and are usually not felt by humans (Table 1). Only 20 earthquakes, on average, exceed a magnitude 7.0 each year. An earthquake that exceeds a magnitude 7.0 is considered to be a major earthquake and serious damage could result.

Earthquakes tend to occur in belts or zones. For example, narrow belts of earthquake epicenters coincide with oceanic ridges where plates separate, such as in the mid-Atlantic and east Pacific Oceans. Earthquakes also occur where plates collide and/or slide past each other. Although most earthquakes originate at plate boundaries, a small percentage occur within plates. The New Madrid earthquakes of 1811–12 are examples of large and destructive intraplate earthquakes in the United States.

The New Madrid earthquakes of 1811 and 1812 are probably the earliest historical earthquake tremors felt in Oklahoma (Arkansas Territory) by residents in southeastern Oklahoma settlements. Before Oklahoma became a state, the earliest documented earthquake occurred October 22, 1882, probably near Fort Gibson, Indian Territory, although it cannot be located precisely (Ross, 1882; Indian Pioneer Papers, date unknown). The *Cherokee Advocate* newspaper reported that at Fort Gibson "the trembling and vibrating were so severe as to cause doors and window shutters to open and shut, hogs in pens to fall and squeal, poultry to run and hide, the tops of weeds to dip, [and] cattle to lowe" (Ross, 1882, p. 1). These observations indicate MM-VIII intensity effects. The next documented earthquake in Oklahoma occurred near Jefferson, Grant County, on December 2, 1897 (Stover and others, 1981). The next known Oklahoma earthquake happened near Cushing, Payne County, in December 1900. This event was followed by two additional earthquakes in the same area in April 1901 (Wells, 1975).

The largest known Oklahoma earthquake (with the possible exception of the 1882 earthquake) occurred near El Reno, Canadian County, on April 9, 1952. This magnitude-5.5 (mb, Gutenberg-Richter) earthquake was felt in Austin, Texas, as well as Des Moines, Iowa, and covered a felt area of ~362,000 km^2 (Docekal, 1970; Kalb, 1964; von Hake, 1976). From 1897 through 1998, 1,557 earthquakes have been located in Oklahoma.

Instrumentation

A statewide network of 10 seismograph stations was used to locate 68 earthquakes in Oklahoma for 1998 (Fig. 1). Station UYO was closed on January 5, 1998. The Oklahoma Geological Survey (OGS) Observatory station, TUL, located near Leonard, Oklahoma, in southern Tulsa County, records 15 continuous seismic signals from sensors located at four stations. The data are recorded, analyzed, and archived on a

[1]Oklahoma Geological Survey Observatory, Leonard.
[2]Oklahoma Geological Survey.

TABLE 1. — ESTIMATED NUMBER OF WORLDWIDE EARTHQUAKES PER YEAR BY MAGNITUDE
(Modified from Tarbuck and Lutgens, 1990)

Magnitude	Estimated number per year	Earthquake effects
<2.5	>900,000	Generally not felt, but recorded
2.5–5.4	30,000	*Minor to moderate earthquakes* Often felt, but only minor damage detected
5.5–6.0	500	*Moderate earthquakes* Slight damage to structures
6.1–6.9	100	*Moderate to major earthquakes* Can be destructive in populous regions
7.0–7.9	20	*Major earthquakes* Inflict serious damage if in populous regions
≥8.0	1–2	*Great earthquakes* Produce total destruction to nearby communities

GSE digital seismic system provided by the Defense Advanced Research Projects Agency/Nuclear Monitoring Research Office.

Signals are digitized by one Geotech RDAS (Remote Data Acquisition System) unit at either 3,600 or 1,200 24-bit samples per second. The RDAS then applies digital anti-alias filtering to eliminate frequencies too high for the final sampling rate. After one to three digital filter and resampling stages, the RDAS produces 60, 40, 20, or 10 24-bit samples per second. The samples are time-tagged by RDAS clocks locked to low-frequency time signals from National Institute of Standards and Technology station WWVB. The signals are passed by RS422 serial links to an AST 386/25 RTDS (Real Time Data Server) computer, which has a Lynx™ real-time Unix-like operating system. The partially processed signals are passed by ethernet to a Sun SPARC 2+ Unix workstation with 64 megabytes of memory, two 660-megabyte disks, two 2.1-gigabyte disks, and two 2.5 gigabyte Exabyte™ tape drives. All of the data from the most recent two weeks are retained on disk. Each day, data from the preceding day (167 million bytes) are automatically archived onto Exabyte tape. All Oklahoma earthquakes, and other selected events, are placed in named de-archive directories on disk. An Oracle™ data base on the Sun SPARC 2+ keeps track of every second of data on the permanent archive tapes, the last 14 days' data on disk, and data in the de-archive directories. Data analysis is done by Teledyne-Geotech and Science Applications International Corp. software on the SPARC 2+ workstation.

The digital system signals are from three sensors in the Observatory vault (international station abbreviation TUL); from a three-component broadband sensor in

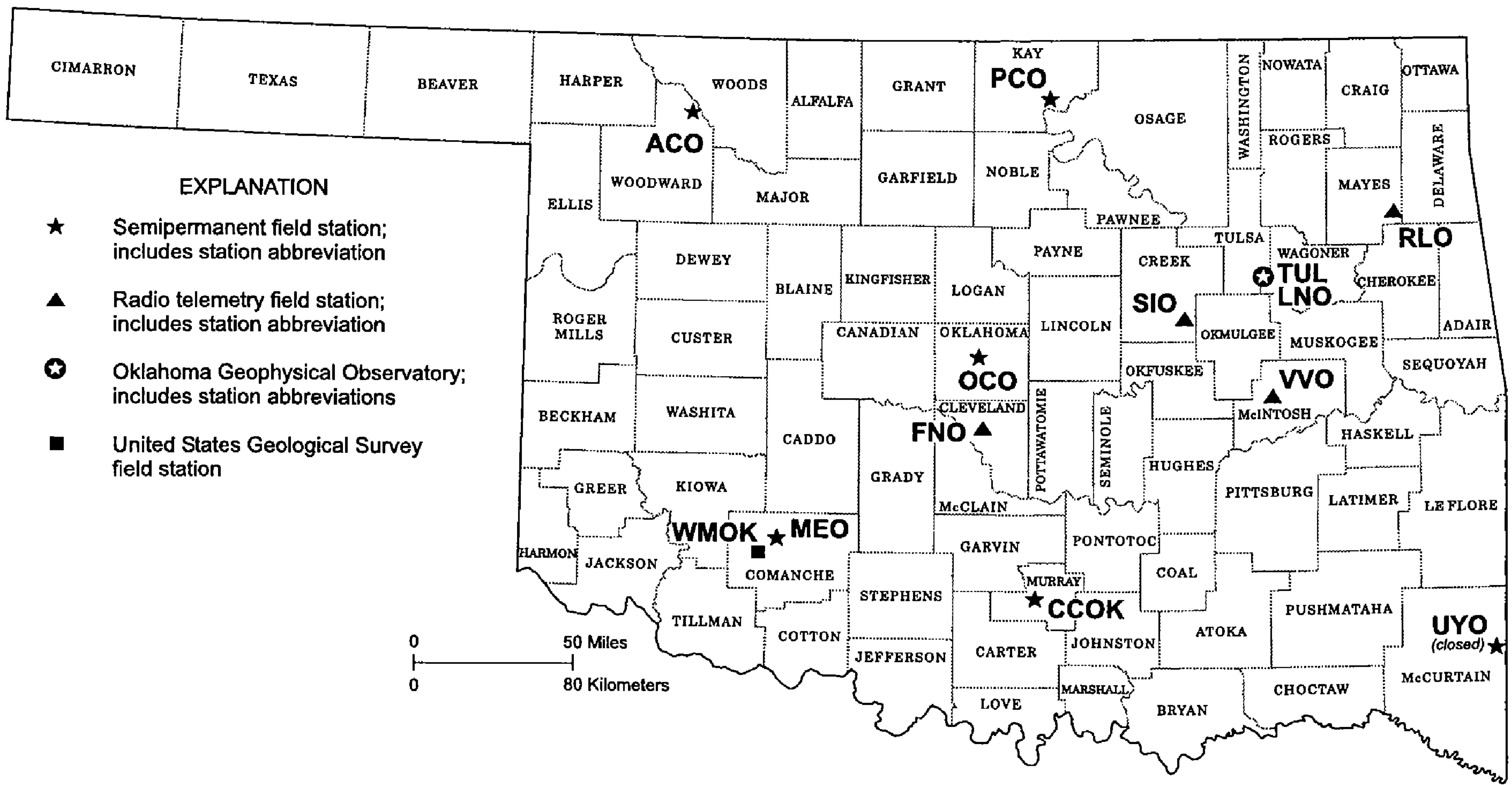

Figure 1. Active seismographs in Oklahoma.

a 120-m borehole; and from single sensors located at Rose Lookout (RLO) in Mayes County, at the Bald Hill Ranch near Vivian (VVO) in McIntosh County, and at the Jackson Ranch near Slick (SIO) in Creek County.

TUL has three (vertical, north–south, east–west) Geotech GS-13 seismometers that produce 40-sample-per-second short-period signals. A three-component broadband Geotech KS54000-0103 seismometer in a 120-m-deep borehole produces seven digital data channels. Three are broadband signals from seismic signals in vertical, north–south, and east–west directions. From the broadband signals the SPARC 2+ workstation derives three long-period signals. A seventh signal, the vertical earth tides, is recorded from the vertical mass displacement signal from the KS54000-0103. The broadband signals are archived at 10 samples per second, and the long-period and vertical-earth-tide signals are recorded at 1 sample per second. On November 10, 1994, the broadband sample rate was increased from 10 samples per second to 20 samples per second. This increase was for two purposes. One was to allow the broadband borehole seismometer to record higher frequencies characteristic of Oklahoma earthquakes. The other was to make the signals compatible for the GSETT-3 (Group of Scientific Experts Technical Test-3), which began in 1995. GSETT-3 is a prototype international seismic-monitoring system to detect underground nuclear tests. Data segments will be copied automatically and sent to the International Data Center by Internet without affecting the recording and analysis of Oklahoma earthquakes.

Through Department of Defense funding (DEPSCoR) the OGS has added a second digital system at Leonard. It consists of a Guralp CMG-3TD three-component (vertical, north–south, and east–west earth motion) broadband (10 microhertz to 90 hertz) seismometer at a depth of 830 m in a borehole. The output of each component is sampled 2,000 times per second by computer elements inside the seismometer case. The 2,000-sample-per-second streams are digitally filtered and decimated to produce three output streams at 200, 20, and 4 samples per second. These streams are sent to the surface and overland to the Observatory by optical fiber. Optical fiber also sends GPS (Global Positioning System satellite) time signals downhole to the computer in the seismometer.

The optical signals are decompressed and archived by an IBM-compatible computer with Guralp Scream software. The four-hour-long data files are transferred to a Sun SPARC20 computer, where they are analyzed by two seismic software packages: SAC2000, developed by Lawrence Livermore National Lab, and GeoTool, developed by Defense Advanced Research Projects Agency.

The 200-sample-per-second streams from the Guralp seismometer have allowed us to see signals from Oklahoma earthquakes up to 90 hertz. With the older system (40 samples per second), 16 hertz was the upper limit. Ninety hertz energy from the April 28 magnitude 4.2 earthquake may be seen on the spectrogram at the Internet address http://www.okgeosurvey1.gov/level2/ok.grams/K980428hzlzne.html.

RLO, VVO, and SIO have Geotech S-13 seismometers in shallow tank vaults. The seismic signals are amplified and used to frequency modulate an audio tone that is transmitted to Leonard with 500-mW FM transmitters at various frequencies in the 216–220-mHz band. The signals are received by antennas on a 40-m-high tower at Leonard; the tones are discriminated to produce a voltage that is proportional to the remote seismometer voltage; and the voltages are digitized at 40 samples per second by the vault RDAS.

A fourth radio-telemetry station, FNO, was installed in central Oklahoma on April 28, 1992, in Norman. The seismometer, Geotech S-13, is on a concrete pad, ~7 km northeast of Sarkeys Energy Center (the building that houses the OGS main office). A discriminator converts the audio-signal frequency fluctuations to a voltage output. The voltage-output is amplified and recorded by a Sprengnether MEQ-800 seismograph recorder (located in an OGS display case) at 60 mm/min trace speed.

Oklahoma earthquake catalogs, earthquake maps, some seismograms, and related information are on the Internet at http://www.okgeosurvey1.gov

In the Leonard vault, seven additional seismometers produce analog (wiggly-line) recordings on paper-drum recorders. Eleven such recordings are produced, five of which are the proper frequencies to record some aspect of nearby earthquakes. One paper recording is produced from each of RLO, VVO, and SIO. The paper records are used as a digital system backup, and to scan for earthquakes faster than is possible on computer screens.

In addition to the digital and analog seismograms recorded at the OGS Observatory and main office, seismograms are recorded by five volunteer-operated seismographs. Each consists of a Geotech S-13 short-period vertical-motion-sensing seismometer in a shallow tank vault, or in an abandoned mine shaft (station MEO) or large-diameter, hand-dug, shallow water well (station CYO). The seismometer signal runs through 200–1,800 ft of cable in surface PVC conduit to the volunteer's house or other building. The volunteer has a Sprengnether MEQ-800B timing system amplifier-filter-drum recorder, which records 24 hours of seismic trace at 1 mm/min in a spiral path around the paper on the drum. The times are set by a time signal radio receiver tuned to the National Institute of Standards and Technology and high-frequency radio station WWV. The volunteers mail the seismograms to the Observatory weekly (or more often, if requested). When an earthquake is felt in Oklahoma, the volunteer operators fax seismogram copies to the Observatory so that the earthquake can be located rapidly.

Station OCO, which contains equipment similar to the volunteer-operated stations, is located at the Omniplex museum in Oklahoma City. Omniplex staff members change the seismic records daily as well as maintain the equipment. OGS Observatory staff help interpret the seismic data and archive the seismograms with all other Oklahoma network seismograms.

The U.S. Geological Survey established a seismograph station 19 km from the OGS station at MEO at Meers. WMOK, the USGS station, does not record continuously. When triggered by moderately strong ground motion it transmits a short segment of data to the National Earthquake Information Service in Golden, Colorado. WMOK is used mostly for distant earthquakes, although it sometimes records some of the larger Oklahoma earthquakes. Because WMOK is so near MEO, its arrival times do not improve the accuracy of location of Oklahoma earthquakes.

Data Reduction and Archiving

In previous years, data processing was done by a series of manual steps, with earthquake locations calculated on a Hewlett-Packard 9825T desktop programmable calculator. This procedure has been in transition to processing on networked Sun Unix workstations.

All network digital and analog short-period (frequencies above about 1 hertz) and broadband seismograms are scanned for earthquakes in and near Oklahoma. The arrival times of P and S phases are recorded on a single-page form in a looseleaf notebook. The arrivals then are entered into the SPARC20 or the SPARC 2+ using a user-friendly flexible program written in the Nawk language. The program uses the entries to write an input file with a unique file name; for example, "hyposat-in.199804011555" would be the name for input data for an earthquake occurring on April 1, 1998, within a minute of 1155 GMT/UTC. The use of a four-digit year will allow for earthquakes in the year 2000 and after.

From the input files, the hypocenters are located by Johannes Schweitzer's (1997) program HYPOSAT 3.2c. A Nawk program manages the input to HYPOSAT and puts the output in a single file (e.g., hyposat-out.199804011555.C) and writes a line in an overall catalog file.

HYPOSAT must have a velocity model of the crust and top of the mantle to calculate travel times of P and S to each station from each successive hypocenter tried in the program. Fifteen solutions, using four different models, were tried on each 1998 earthquake. The nine-layer-plus-upper-mantle Chelsea model for Oklahoma proved the best. This model was derived by Mitchell and Landisman (1971). This model and three other Oklahoma models are outlined on the Observatory Web site at http://www.okgeosurvey1.gov/level2/geology/ok.crustal.models.html.

In the past, almost all earthquakes had to have hypocentral depth restrained at 5.0 km. Of 1998's 68 earthquakes, five were located by last year's methods, because HYPOSAT would not find a solution. HYPOSAT has a real possibility of finding an accurate depth, and it did for 32 of the earthquakes. However, HYPOSAT restrained depth at 5.0 km for 26 earthquakes, and at other depths for six earthquakes.

Each hypocenter is usually run in a preliminary form using the first four or so P and/or S arrivals from about four stations. Later, after all seismograms have been read, a final location is determined. The solutions are added manually to a catalog on the Observatory Web site at http://www.okgeosurvey1.gov/level2/okeqcat/okeqcat.1998.html.

Earthquake Distribution

All Oklahoma earthquakes recorded on seismograms from three or more stations are located. In 1998, 68 Oklahoma earthquakes were located (Figs. 2, 3; Table 2). Three earthquakes were reported felt (Table 3). The felt and observed effects of earthquakes generally are given values according to the Modified Mercalli intensity scale, which assigns a Roman numeral to each of 12 levels described by effects on humans, man-made constructions, or natural features (Table 4).

On April 28 at 9:13 a.m. (local time), a magnitude 4.2 (m3Hz) earthquake occurred 9 km west of Richards Spur in Comanche County. This earthquake caused some damage near Medicine Park and north and east of Lake Lawtonka. The felt areas, approximately 15,750 km^2, extended north to Pawnee, west to Greer County, and south and east to the outskirts of Dallas, Texas.

Two small earthquakes were reported felt, one in Wagoner County on October 25, and the other in Grant County on October 30. Both earthquakes produced MM-IV effects near the epicenter. The felt areas for both earthquakes are probably re-

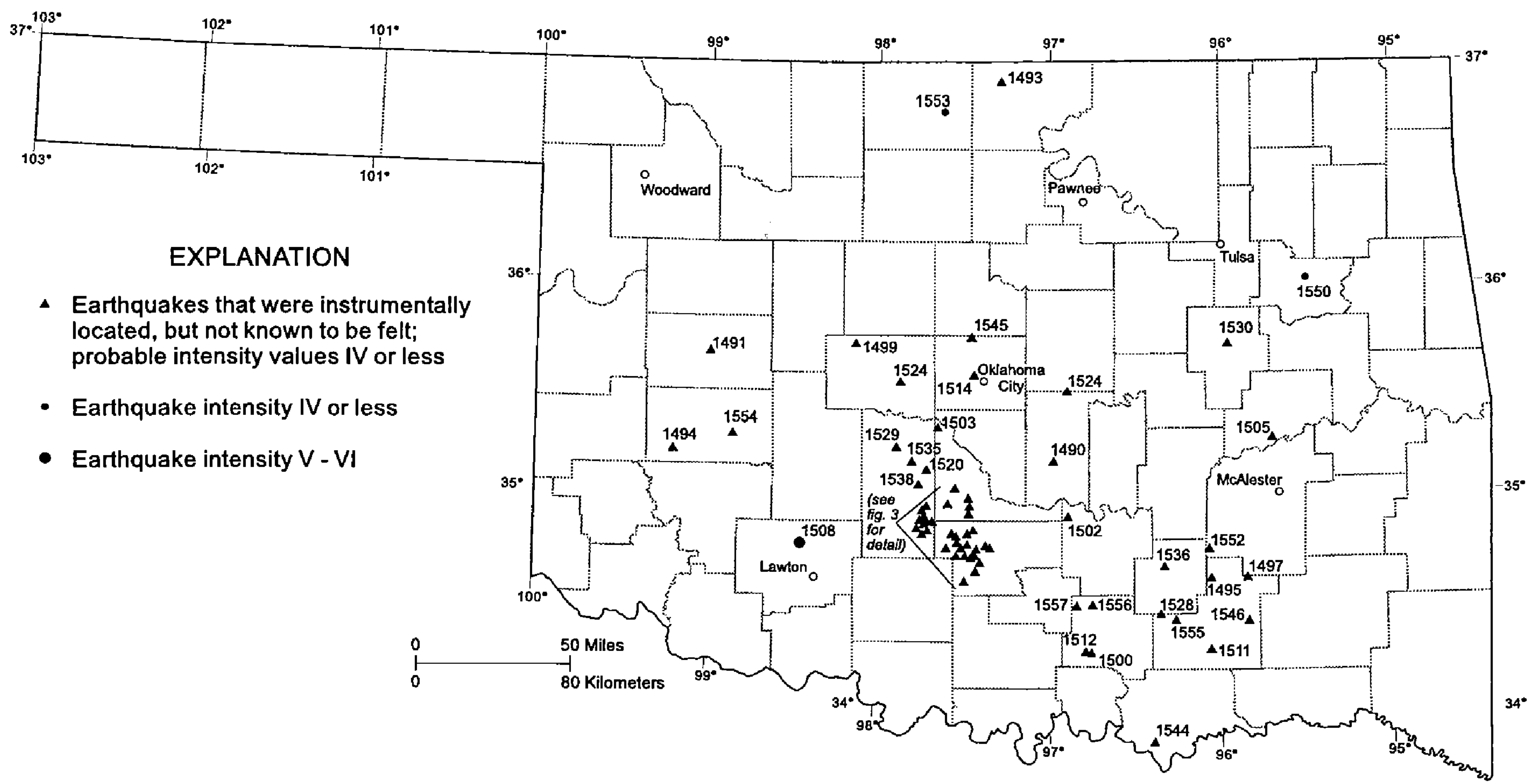

Figure 2. Distribution of Oklahoma earthquakes for 1998. Numbers correspond to event numbers in Table 2.

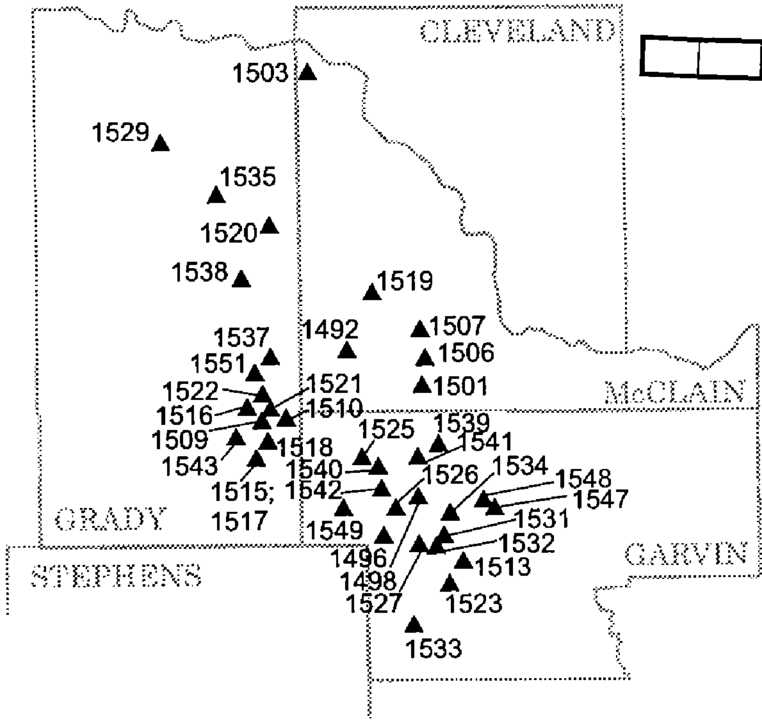

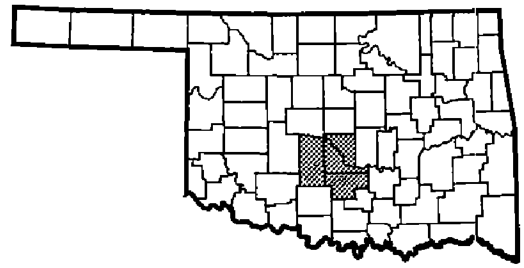

▲ Earthquakes that were instrumentally located, but not known to be felt; probable intensity values IV or less

Figure 3. Distribution of 1998 earthquakes, Grady, McClain, and Garvin Counties, Oklahoma. Numbers correspond to event numbers in Table 2.

stricted to a few tens of square kilometers from the epicentral locations. No damage was reported from these events.

Earthquake-magnitude values ranged from a low of 0.9 (MDUR) in Okmulgee County to a high of 4.2 (mbLg) in Comanche County. More than half (39) of the 1998 locatable earthquakes occurred in Garvin, Grady, and McClain Counties. Johnston and Atoka Counties each experienced four earthquakes; Canadian, Coal, Pittsburg, Pottawatomie, and Washita Counties each had two.

Catalog

For both preliminary and final locations, the catalog of Oklahoma earthquakes is in HTML (World Wide Web) format; one HTML page contains all the earthquakes that occurred in one year (a single page lists earthquakes for multiple years prior to 1977). In order to assure absolute uniformity, the catalog is stored only in HTML format. One copy is on a Sun SPARC20 at the Observatory in Leonard, and a second copy is on a ONENet server in Tulsa. ONENet is the network of the Oklahoma Regents for Higher Education. The server copy, at the World Wide Web address http://www.okgeosurvey1.gov, is used for both public distribution and in-house reference; the Observatory copy is a backup copy.

A Perl-language program searches the catalog for all of the earthquakes occurring in a given year, and will do narrower searches. Searches can be done, for example, for all earthquakes within a given circle or rectangle, for all earthquakes in a given county, for earthquakes occurring within a particular time interval, for felt-only earthquakes, and for earthquakes of a minimum magnitude. At present the capability for selective searches is available only to Observatory users, but in late 1999 the search program will be available on the World Wide Web.

Each event in the catalog is sequentially numbered and arranged according to date and origin time. The numbering system is compatible with the system used by

TABLE 2. — OKLAHOMA EARTHQUAKE CATALOG FOR 1998

Event no.	Date and origin time (UTC)[a]		County	Intensity MM[b]	Magnitudes 3Hz	bLg	DUR	Latitude deg N	Longitude deg W	Depth (km)[c]
1490	Jan 01	20 26 54.20	Pottawatomie		2.2	2.1	2.0	35.142	96.981	10.3 C
1491	Jan 06	10 16 36.20	Custer		2.0	1.9	2.4	35.643	98.999	0.0R C
1492	Jan 21	01 35 54.40	McClain		1.4	1.6	1.7	34.932	97.599	5.0 C
1493	Jan 26	06 57 31.79	Kay		1.6		1.8	36.903	97.290	5.0R C
1494	Feb 15	08 53 42.95	Washita				2.1	35.191	99.209	5.0R C
1495	Feb 18	10 59 42.22	Atoka		1.1		1.1	34.583	96.063	5.0R C
1496	Mar 02	09 09 37.93	Garvin		1.7	1.6	1.7	34.693	97.536	3.3 C
1497	Mar 08	09 28 57.18	Pittsburg		1.4		1.5	34.598	95.850	5.0 C
1498	Mar 18	15 46 44.38	Garvin		2.1	1.8	1.7	34.738	97.480	5.0R C
1499	Mar 18	16 06 34.41	Canadian			1.6		35.681	98.136	5.0R N
1500	Mar 18	22 33 22.71	Johnston				1.8	34.234	96.767	8.0 C
1501	Mar 22	02 12 35.81	McClain		2.0	1.8	1.6	34.893	97.478	8.2 C
1502	Mar 22	12 22 49.98	Pontotoc		1.5		1.2	34.870	96.900	7.2 C
1503	Apr 01	15 55 14.52	McClain				1.8	35.292	97.658	0.2R C
1504	Apr 01	19 50 30.86	Canadian				1.7	35.512	97.870	5.0R C
1505	Apr 01	23 26 34.59	McIntosh		1.7	1.6	1.9	35.239	95.701	25.1 C
1506	Apr 02	07 10 32.98	McClain				2.1	34.923	97.476	2.0 C
1507	Apr 08	13 34 17.12	McClain				1.9	34.957	97.478	2.6 C
1508	Apr 28	14 13 01.27	Comanche	6	4.2			34.755	98.447	5.0R C
1509	May 02	16 12 04.11	Grady		2.3	2.2	1.9	34.841	97.728	7.1 C
1510	May 02	16 55 44.44	Grady		2.2	1.6	1.7	34.850	97.691	3.1 C
1511	May 02	23 56 04.79	Atoka		2.2	1.9	1.9	34.252	96.059	15.2 C
1512	May 04	23 04 53.83	Johnston				1.7	34.243	96.791	0.7 C
1513	Jun 02	06 29 32.27	Garvin				1.7	34.660	97.415	16.3 C
1514	Jun 12	09 45 59.44	Oklahoma				1.8	35.541	97.445	5.0R C
1515	Jun 30	17 10 44.18	Grady				1.8	34.800	97.741	5.0R N
1516	Jun 30	17 32 07.05	Grady		2.3		1.8	34.852	97.740	6.2 C
1517	Jul 01	00 48 23.00	Grady		2.6	2.6	2.3	34.800	97.741	17.7 C
1518	Jul 01	08 51 37.53	Grady				2.2	34.819	97.721	9.1 C
1519	Jul 01	17 29 38.86	McClain				2.0	35.006	97.553	5.0R C
1520	Jul 02	00 46 52.38	Grady				2.0	35.092	97.725	5.0R C
1521	Jul 02	09 04 20.26	Grady				2.3	34.855	97.726	5.0R C
1522	Jul 02	21 21 31.53	Grady				2.1	34.865	97.731	2.8 C
1523	Jul 07	18 44 44.35	Garvin				2.5	34.629	97.430	0.1 C
1524	Jul 07	23 39 48.98	Pottawatomie				1.8	35.460	96.904	5.0R N
1525	Jul 09	14 45 36.19	Garvin				1.9	34.791	97.572	5.7 C
1526	Jul 09	16 44 44.02	Garvin				2.1	34.735	97.519	5.0R C
1527	Jul 09	22 10 27.75	Garvin				2.2	34.684	97.478	5.0R C
1528	Jul 14	03 26 28.37	Coal				2.0	34.422	96.352	5.0R C
1529	Jul 22	10 04 18.66	Grady				1.8	35.196	97.886	10.2 C
1530	Aug 03	06 39 10.62	Okmulgee		1.0		0.9	35.687	95.959	5.0R C
1531	Aug 03	18 09 34.01	Garvin		1.6		1.3	34.694	97.448	5.0R C
1532	Aug 03	18 41 40.40	Garvin		1.7		1.6	34.684	97.457	5.0R C
1533	Aug 03	21 15 35.68	Garvin				1.4	34.577	97.493	5.0R N
1534	Aug 03	22 47 44.36	Garvin		1.7		1.6	34.713	97.437	5.3 C
1535	Aug 08	03 45 33.37	Grady		1.5		1.9	35.136	97.803	5.0R C
1536	Aug 13	15 33 51.54	Coal		1.9	1.6	1.6	34.643	96.344	5.8 C
1537	Aug 22	22 05 29.39	Grady		1.6		1.8	34.924	97.718	5.0R C
1538	Aug 23	05 46 04.29	Grady		1.8	1.6	1.7	35.022	97.765	5.9 C
1539	Aug 30	06 25 07.76	Garvin		1.5	1.7	1.6	34.811	97.452	0.9R C
1540	Aug 31	14 01 00.62	Garvin		1.5	1.6	1.5	34.775	97.549	4.3 C
1541	Aug 31	15 58 44.80	Garvin		1.7	1.7	1.8	34.794	97.484	9.4 C
1542	Aug 31	21 07 29.69	Garvin		1.6		1.6	34.759	97.538	5.0R C
1543	Sep 08	17 57 29.12	Grady		1.7	1.8	1.9	34.824	97.773	5.0R C
1544	Sep 15	22 31 29.11	Bryan				1.9	33.815	96.391	5.0R N
1545	Sep 16	04 02 06.43	Logan				1.5	35.724	97.454	5.0R C
1546	Oct 20	09 48 23.09	Atoka				1.6	34.386	95.837	11.6R C
1547	Oct 21	15 14 12.00	Garvin				1.5	34.729	97.363	5.0R C
1548	Oct 21	15 27 50.30	Garvin				1.6	34.731	97.375	1.2R C

Event no.	Date and origin time (UTC)[a]		County	Intensity MM[b]	Magnitudes 3Hz	bLg	DUR	Latitude deg N	Longitude deg W	Depth (km)[c]
1549	Oct 21	16 29 43.66	Garvin				1.7	34.732	97.602	5.0R C
1550	Oct 25	03 48 07.71	Wagoner	4			1.9	35.994	95.493	16.5 C
1551	Oct 29	04 15 00.65	Grady				2.0	34.905	97.734	3.5 C
1552	Oct 29	08 44 19.35	Pittsburg				1.7	34.717	96.074	0.1 C
1553	Oct 30	17 41 21.42	Grant	4			3.5	36.771	97.623	7.8 C
1554	Nov 04	02 26 00.69	Washita				1.9	35.263	98.856	12.8R C
1555	Nov 14	09 03 35.70	Atoka				1.5	34.389	96.273	1.7 C
1556	Dec 07	08 58 30.76	Johnston				1.6	34.467	96.761	5.0R C
1557	Dec 15	21 29 29.26	Johnston				1.7	34.457	96.849	6.6 C

[a]UTC refers to Coordinated Universal Time, formerly Greenwich Mean Time. The first two digits refer to the hour on a 24-hour clock. The next two digits refer to the minute, and the remaining digits are the second. To convert to local Central Standard Time, subtract 6 hours.

[b]Modified Mercalli (MM) earthquake-intensity scale (see Table 4).

[c]5.0R indicates that the depth was restrained to 5.0 km from the beginning of the calculation. If R is preceded by a number other than 5.0, the depth was restrained at that depth part way through the location calculations. When R does not appear, the number was an unrestrained depth, readjusted at every iteration during the location. N refers to the Nuttli velocity model; C refers to the Chelsea velocity model.

Lawson and Luza (1980–90, 1993–98), Lawson and others (1991, 1992), and for the *Earthquake Map of Oklahoma* (Lawson and Luza, 1995b). The Oklahoma earthquakes article published annually in *Oklahoma Geology Notes* uses an additional sequential number not found on the World Wide Web catalog.

The dates and times for the cataloged earthquakes are given in UTC. UTC refers to Coordinated Universal Time, formerly Greenwich Mean Time. The first two digits refer to the hour on a 24-hour clock. The next two digits refer to the minute, and the remaining digits are the seconds. To convert to local Central Standard Time, subtract 6 hours.

Earthquake magnitude is a measurement of energy and is based on data from seismograph records. The magnitude of a local earthquake is determined by taking the logarithm (base 10) of the largest ground motion recorded during the arrival of a seismic-wave type and applying a standard correction for distance to the epicenter. When the magnitude value is increased one unit, the amplitude of the earthquake waves increases 10 times. There are several different scales used to report magnitude. Table 2 has three magnitude scales, which are mbLg (Nuttli), m3Hz (Nuttli), and MDUR (Lawson). Each magnitude scale was established to accommodate specific criteria, such as the distance from the epicenter, as well as the availability of certain seismic data.

For earthquake epicenters located 11–222 km from a seismograph station, Otto Nuttli developed the m3Hz magnitude scale (Zollweg, 1974). This magnitude is derived from the following expression:

$$m3Hz = \log(A/T) - 1.63 + 0.87 \log(\Delta),$$

where A is the maximum center-to-peak vertical-ground-motion amplitude sustained for three or more cycles of Lg waves, near 3 Hz in frequency, measured in nanometers; T is the period of the Lg waves measured in seconds; and Δ is the great-circle distance from epicenter to station measured in kilometers.

In 1979, St. Louis University (Stauder and others, 1979) modified the formulas for m3Hz. This modification was used by the OGS Observatory beginning January 1, 1982. The modified formulas had the advantage of extending the distance range

TABLE 3. — EARTHQUAKES REPORTED FELT IN OKLAHOMA, 1998

Event no.	Date and origin time (UTC)[a]		Nearest city	County	Intensity MM[b]
1508	Apr 28	14 13 01.27	9 km W Richards Spur	Comanche	6
1550	Oct 25	03 48 07.71	15 km NW Wagoner	Wagoner	4
1553	Oct 30	17 41 21.42	10 km SE Medford	Grant	4

[a]UTC refers to Coordinated Universal Time, formerly Greenwich Mean Time. The first two digits refer to the hour on a 24-hour clock. The next two digits refer to the minute, and the remaining digits are the second. To convert to local Central Standard Time, subtract 6 hours.

[b]Modified Mercalli (MM) earthquake-intensity scale (see Table 4).

for measurement of m3Hz out to 400 km, but also had the disadvantage of increasing m3Hz by about 0.12 units compared to the previous formula. Their formulas were given in terms of $\log(A)$ but were restricted to wave periods of 0.2–0.5 sec. In order to use $\log(A/T)$, we assumed a period of 0.35 sec in converting the formulas for our use. The resulting equations are:

(epicenter 10–100 km from a seismograph)

$$\text{m3Hz} = \log(A/T) - 1.46 + 0.88 \log(\Delta)$$

(epicenter 100–200 km from a seismograph)

$$\text{m3Hz} = \log(A/T) - 1.82 + 1.06 \log(\Delta)$$

(epicenter 200–400 km from a seismograph)

$$\text{m3Hz} = \log(A/T) - 2.35 + 1.29 \log(\Delta).$$

Otto Nuttli's (1973) earthquake magnitude, mbLg, for seismograph stations located between 55.6 and 445 km from the epicenter, is derived from the following equation:

$$\text{mbLg} = \log(A/T) - 1.09 + 0.90 \log(\Delta).$$

Where seismograph stations are located between 445 and 3,360 km from the epicenter, mbLg is defined as:

$$\text{mbLg} = \log(A/T) - 3.10 + 1.66 \log(\Delta),$$

where A is the maximum center-to-peak vertical-ground-motion amplitude sustained for three or more cycles of Lg waves, near 1 Hz in frequency, measured in nanometers; T is the period of Lg waves measured in seconds; and Δ is the great-circle distance from epicenter to station measured in kilometers.

The MDUR magnitude scale was developed by Lawson (1978) for earthquakes in Oklahoma and adjacent areas. It is defined as:

$$\text{MDUR} = 1.86 \log(\text{DUR}) - 1.49,$$

where DUR is the duration or difference, in seconds, between the Pg-wave arrival time and the time the final coda amplitude decreases to twice the background-noise amplitude. Before 1981, if the Pn wave was the first arrival, the interval between the earthquake-origin time and the decrease of the coda to twice the background-noise amplitude was measured instead. Beginning January 1, 1982, the interval

TABLE 4. — MODIFIED MERCALLI (MM) EARTHQUAKE-INTENSITY SCALE
(Abridged) (Modified from Wood and Neumann, 1931)

I	Not felt except by a very few under especially favorable circumstances.
II	Felt only by a few persons at rest, especially on upper floors of buildings. Suspended objects may swing.
III	Felt quite noticeably indoors, especially on upper floors of buildings. Automobiles may rock slightly.
IV	During the day felt indoors by many, outdoors by few. At night some awakened. Dishes, doors, windows disturbed. Automobiles rocked noticeably.
V	Felt by nearly everyone, many awakened. Some dishes, windows, etc., broken; unstable objects overturned. Pendulum clocks may stop.
VI	Felt by all; many frightened and run outdoors.
VII	Everybody runs outdoors. Damage negligible in buildings of good design and construction. Shock noticed by persons driving automobiles.
VIII	Damage slight in specially designed structures; considerable in ordinary substantial buildings; great in poorly built structures. Fall of chimneys, stacks, columns. Persons driving automobiles disturbed.
IX	Damaged considerable even in specially designed structures; well-designed frame structures thrown out of plumb. Buildings shifted off foundations. Ground cracked conspicuously.
X	Some well-built wooden structures destroyed; ground badly cracked, rails bent. Landslides and shifting of sand and mud.
XI	Few if any (masonry) structures remain standing. Broad fissures in ground.
XII	Damage total. Waves seen on ground surfaces.

from the beginning of the P wave (whether it was Pg, P*, or Pn) to the decrease of the coda to twice the background-noise amplitude was used.

Earthquake detection and location accuracy have been greatly improved since the installation of the statewide network of seismograph stations. The frequency of earthquake events and the possible correlation of earthquakes to specific tectonic elements in Oklahoma are being studied. It is hoped that this information will provide a more complete data base that can be used to develop numerical estimates of earthquake risk, giving the approximate frequency of the earthquakes of any given size for various regions of Oklahoma. Numerical risk estimates could be used for better design of large-scale structures, such as dams, high-rise buildings, and power plants, as well as to provide the necessary information to evaluate insurance rates.

Acknowledgments

Shirley Jackson (retired July 28, 1998, after 20 years of service), Todd McCormick, and James King (appointed April 28) maintained the OGS Observatory at Leonard.

Volunteer seismograph-station operators and landowners at various locations in Oklahoma make possible the operation of a statewide seismic network.

This work was funded directly by the Oklahoma Geological Survey. The GSE digital seismic system, provided by the Defense Advanced Research Projects Agency/ Nuclear Monitoring Research Office, considerably enhanced the OGS's ability to analyze Oklahoma earthquakes. A borehole seismic system, a joint project with the Lawrence Livermore National Laboratories, was useful in recording Oklahoma earthquakes. The three-component broadband Guralp seismometer in the 830-m borehole and the Guralp data aquisition system were funded by a DARPA-DEPSCoR grant. The Observatory exists because of building and land-purchase gifts from Jersey Production Research Co. (now merged into Exxon) and the Sarkeys Foundation.

References Cited

Docekal, Jerry, 1970, Earthquakes of the stable interior, with emphasis on the Midcontinent: University of Nebraska, Lincoln, unpublished Ph.D. dissertation, v. 1, 169 p.; v. 2, 332 p.

Indian Pioneer Papers [date unknown], Interview, Eliza Ross: Western History Collections, University of Oklahoma Libraries, Norman, v. 78, p. 164–167.

Kalb, Bill, 1964, Earthquakes that shook Oklahoma: Orbit Magazine—The Sunday Oklahoman, Oklahoma City, September 27, p. 4–7.

Lawson, J. E., Jr., 1978, A preliminary duration magnitude scale for local and regional earthquakes recorded at Oklahoma seismograph stations: Oklahoma Geological Survey Observatory Open-File Report, 14 p.

_____ 1980, Geophysical observatory establishes continuous time synchronization: Oklahoma Geology Notes, v. 40, p. 214.

Lawson, J. E., Jr.; and Luza, K. V., 1980, Oklahoma earthquakes, 1979: Oklahoma Geology Notes, v. 40, p. 95–105.

_____ 1981, Oklahoma earthquakes, 1980: Oklahoma Geology Notes, v. 41, p. 140–149.

_____ 1982, Oklahoma earthquakes, 1981: Oklahoma Geology Notes, v. 42, p. 126–137.

_____ 1983, Oklahoma earthquakes, 1982: Oklahoma Geology Notes, v. 43, p. 24–35.

_____ 1984, Oklahoma earthquakes, 1983: Oklahoma Geology Notes, v. 44, p. 32–42.

_____ 1985, Oklahoma earthquakes, 1984: Oklahoma Geology Notes, v. 45, p. 52–61.

_____ 1986, Oklahoma earthquakes, 1985: Oklahoma Geology Notes, v. 46, p. 44–52.

_____ 1987, Oklahoma earthquakes, 1986: Oklahoma Geology Notes, v. 47, p. 65–72.

_____ 1988, Oklahoma earthquakes, 1987: Oklahoma Geology Notes, v. 48, p. 54–63.

_____ 1989, Oklahoma earthquakes, 1988: Oklahoma Geology Notes, v. 49, p. 40–48.

_____ 1990, Oklahoma earthquakes, 1989: Oklahoma Geology Notes, v. 50, p. 68–76.

_____ 1993, Oklahoma earthquakes, 1992: Oklahoma Geology Notes, v. 53, p. 51–62.

_____ 1994, Oklahoma earthquakes, 1993: Oklahoma Geology Notes, v. 54, p. 57–68.

_____ 1995a, Oklahoma earthquakes, 1994: Oklahoma Geology Notes, v. 55, p. 51–63.

_____ 1995b, Earthquake map of Oklahoma (earthquakes shown through 1993): Oklahoma Geological Survey Map GM-35, scale 1:500,000.

_____ 1996, Oklahoma earthquakes, 1995: Oklahoma Geology Notes, v. 56, p. 49–63.

_____ 1997, Oklahoma earthquakes, 1996: Oklahoma Geology Notes, v. 57, p. 40–52.

_____ 1998, Oklahoma earthquakes, 1997: Oklahoma Geology Notes, v. 58, p. 60–72.

Lawson, J. E., Jr.; Luza, K. V.; and Moss, Dan, 1991, Oklahoma earthquakes, 1990: Oklahoma Geology Notes, v. 51, p. 50–61.

Lawson, J. E., Jr.; Luza, K. V.; Brown, R. L.; and Moss, Dan, 1992, Oklahoma earthquakes, 1991: Oklahoma Geology Notes, v. 52, p. 48–59.

Luza, K. V., 1978, Regional seismic and geologic evaluations of Nemaha uplift, Oklahoma,

Kansas, and Nebraska: Oklahoma Geology Notes, v. 38, p. 49–58.
Mitchell, B. J.; and Landisman, M., 1971, Geophysical measurements in the Southern Great Plains, the structure and physical properties of the Earth's crust: American Geophysical Union Geophysical Monograph 14, p. 77–93.
Mykkeltveit, Svein; Ringdal, Frode; Kvaerna, Tormad; and Alewine, R. W., 1990, Application of regional arrays in seismic verification: Seismological Society of America Bulletin, v. 80, p. 1777–1801.
Nuttli, O. W., 1973, Seismic wave attenuation and magnitude relations for eastern North America: Journal of Geophysical Research, v. 78, p. 876–885.
Ross, D. H. (ed.), 1882, Shake: Cherokee Advocate, Friday, October 27, p. 1.
Schweitzer, Johannes, 1997, HYPOSAT—a new routine to locate seismic events: NORSAR Science Reports, 1-97/98, November 1997, p. 94–102.
Stauder, W.; Hermann, R.; Singh, S.; Reidy, D.; Perry, R.; and Morrissey, Sean-Thomas, 1979, Central Mississippi Valley Earthquake Bulletin: First Quarter 1979, no. 19, 50 p.
Stover, C. W.; Reagor, B. G.; Algermissen, S. T.; and Lawson, J. E., Jr., 1981, Seismicity map of the State of Oklahoma: U.S. Geological Survey Miscellaneous Field Studies Map MF-1352, scale 1:1,000,000.
Tarbuck, E. J.; and Lutgens, F. K., 1990, The earth—an introduction to physical geology: Merrill Publishing Co., Columbus, Ohio, 651 p.
von Hake, C. A., 1976, Earthquake history of Oklahoma: Earthquake Information Bulletin, v. 8, p. 28–30.
Wells, L. L., 1975, Young Cushing in Oklahoma Territory: Frontier Printers, Stillwater, Oklahoma, 221 p.
Wood, H. O.; and Neumann, Frank, 1931, Modified Mercalli intensity scale of 1931: Seismological Society of America Bulletin, v. 21, p. 227–283.
Zollweg, James, 1974, A preliminary study of the seismicity of the central United States, 1974: St. Louis University unpublished undergraduate report, 15 p.

List of OGS Publications for 1999–2000 Now Available

The latest list of in-print OGS publications has been published. For a free copy of the 26-page catalog, contact the Survey at (405) 360-2886; fax: (405) 366-2882; e-mail: ogssales@ou.edu; mailing address: 100 E. Boyd, Room N-131, Norman, OK 73019. Copies are also available over the counter at the OGS Publication Sales Office, 1218-B W. Rock Creek Road, Norman.

Hartshorne Coal Bed, Latimer County *(continued from p. 34)*

nology of the Upper and Lower Hartshorne coals in the same area and noted a 4-in.-thick parting. The discrepancies in the measured thickness of the parting could be due to weathering. The present-day measurement was made by excavating soft, smutty coal back into the exposure until bright coal was found on either side of a 0.5-in.-thick carbonaceous shale parting.

Taylor and others (1998, p. 25) discuss the loss in volume of a coal seam from the peat stage to the bituminous coal stage as a result of compression. It has been suggested that the compaction from peat to bituminous coal is in the proportion of about 6:1—that is, 60 ft of peat will yield ~10 ft of bituminous coal.

It is much more difficult to determine the length of time needed for a given thickness of coal to form, and estimates vary greatly (Taylor and others, 1998, p. 26). A thickness of 10 ft of bituminous coal probably represents accumulation of peat over approximately 18,000–27,000 years.

Reports of subsurface coal beds >10 ft thick must be viewed with great skepticism (at least in Oklahoma). Old drillers' logs on file at the Oklahoma Geological Survey occasionally record coal-bed thicknesses of 20 ft to as much as 45 ft. One must suspect that cutting samples were contaminated with coal chips or that black shale was being logged as coal. Such reports of unrealistically thick coal beds persist into modern times (B. J. Cardott, personal communication, 1999). However, until a reliable observer witnesses cored coal >10 ft thick coming out of the ground in Oklahoma, the Hartshorne coal bed in Latimer County remains the record holder.

References Cited

Russell, D. T., 1960, Geology of northern Latimer County, Oklahoma: Oklahoma Geological Survey Circular 50, 57 p.

Taylor, G. H.; Teichmüller, M.; Davis, A.; Diessel, C. F. K.; Littke, R.; and Robert, P., 1998, Organic petrology: Gebrüder Borntraeger, Berlin, 704 p.

Wilson, L. R., 1970, Palynology of Oklahoma's ten-foot coal seam [abstract]: Geological Society of America Abstracts with Programs, v. 2, no. 4, p. 304–305.

Wood, G. H., Jr.; Kehn, T. M.; Carter, M. D.; and Culbertson, W. C., 1983, Coal resource classification system of the U.S. Geological Survey: U.S. Geological Survey Circular 891, 65 p.

LeRoy A. Hemish

Oil and Gas Education Initiative, June 14–17, 1999, Dallas, Texas. Information: Allen Mesch, Maguire Oil and Gas Institute, Edwin L. Cox School of Business, Southern Methodist University, P.O. Box 750333, Dallas, TX 75275; (214) 768-3693; World Wide Web: www.cox.smu.edu/maguire/ogeibro.html.

International Gemological Symposium, by Gemological Institute of America, June 21–24, 1999, San Diego, California. Information: (800) 421-7250, ext. 4406.

The Future of Coal Bed Methane in the Rocky Mountains, June 22, 1999, Denver, Colorado. Information: Sandi Pellissier, (303) 573-8621, fax-back information: 888-329-4410, document 202.

Bartlesville Play Workshop, cosponsored by Oklahoma City Geological Society and Oklahoma Geological Survey, September 9, 1999, Oklahoma City, Oklahoma. Information: Carol Jones, OCGS, (405) 236-8086, ext. 11.

OGS to Host Workshop on Seismic Exploration

Operators interested in learning whether 2-D or 3-D seismic can benefit their businesses can find out more about these methods at "2-D–3D Seismic: Effective Application Can Improve Your Bottom Line," a one-day workshop to be held on **July 29** at the Frances Tuttle Vo-Tech in Oklahoma City. Cosponsored by the OGS, the Petroleum Technology Transfer Council, and the Marginal Wells Commission, the workshop will give attendees a better understanding of how seismic works, how it can benefit them, when it can best be used, and how much it costs.

The workshop presents a non-mathematical approach to the acquisition, processing, and interpretation of seismic data to give attendees a better feel for when to use seismic methods and what results to expect. Sessions cover the basics of reflection seismic, addressing both 2-D and 3-D seismic methods, and outline the history of seismic exploration technology and its impact on Oklahoma. Case histories in the Midcontinent, West Texas, and Gulf Coast are used as examples.

The main workshop presenters are Deborah King Sacrey, a consulting geologist and owner of Auburn Energy of Houston, who has done a great deal of work in Oklahoma, and Raymon L. Brown, a geophysicist with the Oklahoma Geological Survey.

For more information about the workshop, contact Michelle Summers, OGS, 100 E. Boyd, Room N-131, Norman, OK 73019, telephone (405) 325-3031 or (800) 330-3996, fax (405) 325-7069; or e-mail jlcoleman@ou.edu.

The following abstracts were presented as part of the Geology Section program at the Oklahoma Academy of Science 87th annual technical meeting, Northeastern State University, Tahlequah, November 14, 1998.

Are Porosity and Permeability Fades Selective?—An Example from the Pennsylvanian Cottage Grove Sandstone (Osage-Layton), Cherokee Platform, North-Central Oklahoma

JAMES R. CHAPLIN, Oklahoma Geological Survey, 100 E. Boyd, Room N-131, Norman, OK 73019

Core interpretations indicate that the Cottage Grove Sandstone (Osage-Layton), at least in this geographic setting, is composed primarily of delta-front deposits. The delta-front deposits can be subdivided into a proximal delta-front facies (distributary mouth-bar subfacies) and a distal delta-front facies. The delta-front facies grades seaward into prodelta deposits and is capped by a marine-transgressive black shale facies.

Both porosity and permeability values show a relatively strong correlation with depositional facies and subfacies. Measured core porosity, primarily intergranular and secondarily grain-dissolution types, ranges from 2 to 20%, averaging 16%. Core porosities are consistently higher and more uniform in the upper part of the distributary mouth-bar subfacies and lowest in the distal delta-front, prodelta, and marine-transgressive shale facies. Measured core permeabilities range from 0.007 to 97 md, averaging 15.3 md. The highest permeability measurements were recorded from the proximal delta-front facies (distributary mouth-bar subfacies) and lowest from the distal delta-front, prodelta, and marine-transgressive shale facies.

Clay content, primarily illite + smectite, ranges from 1 to 39%, averaging 18%, and is inversely correlated with grain size. Illite + smectite is the main permeability-reducing component and is followed in decreasing order of importance by quartz overgrowths, ferroan dolomite, and compaction. Grain dissolution of feldspars has generated some secondary porosity.

The primary control on Cottage Grove reservoir quality, at least in this geographic setting, is depositional facies and diagenesis. The proximal delta-front facies is the best reservoir rock, whereas the distal delta-front and prodelta facies have less potential as reservoir rocks because of higher heterogeneity and lower porosity and permeability.

Descriptions of South African Kimberlite-Hosted Eclogites and Alkremites

J. D. DISCHINGER, School of Geology and Geophysics, University of Oklahoma, Norman, OK 73019; *G. HARLOW,* American Museum of Natural History, Central Park West at 79th St., New York, NY 10024; and *G. B. MORGAN VI,* School of Geology and Geophysics, University of Oklahoma, Norman, OK 73019

Eclogite (gt + cpx) and alkremite (gt + sp + cpx) xenoliths were collected from the Jagersfontien kimberlite pipe, South Africa. Electron microprobe analyses indicate that eclogite samples contain pristine pyrope-almandine ($Py_{61.86}Al_{28.40}Gr_{6.32}An_{2.22}$) garnets that are euhedral, to subhedral, 2–4 mm across, and typically orange to honey brown in color. Eclogite clinopyroxene crystals are typically 4–6 mm long and strained. These are diopsitic ($Wo_{42.80}En_{50.60}Fs_{6.60}$) in composition, but minor element abundances suggest there are two populations. Primary clinopyroxene crystals exhibit cleavage fractures that are filled with secondary clinopyroxene. The majority of clinopyroxene occurs as large dark "bottle-glass" green crystals. These are higher in Al and Na with lower abundances of Mg and Ca than the minor white to light green clinopyroxene filling fractures in the larger crystals.

Alkremites contain pristine euhedral pyrope-grossular ($Py_{52.78}Gr_{24.27}Al_{16.01}An_{6.41}$) garnets that are 1–3 mm across and are typically orange to honey brown. Black spinels are commonly found interstitially between garnet grains. Traverses across the spinels show a homogeneous composition of ($Fe^{2+}_{0.23}$, $Mg_{0.76}$)($Fe^{3+}_{0.05}$, $Al_{1.94}$)O_4. Alkremite clinopyroxene occurs along grain boundaries between garnet and spinel. Points analyzed from the clinopyroxene show homogenous diopsitic composition ($Wo_{45.31}En_{44.94}Fs_{9.75}$).

Analyses thus far show that the xenoliths from Jagersfontien underwent varying degrees of alteration. Many examples contain evidence of pervasive metasomatic alteration. Furthermore, the fracture filling texture of the low Al + Mg clinopyroxene in the eclogite suggests that minor amounts of alteration exist in some "pristine" xenoliths.

Permian Geology of the Northern Oklahoma City Metropolitan Area

LEROY A. HEMISH and *NEIL H. SUNESON*, Oklahoma Geological Survey, 100 E. Boyd, Room N-131, Norman, OK 73019

The Oklahoma Geological Survey (OGS) mapped four 7.5-minute quadrangles (Piedmont, Bethany NE, Edmond, and Arcadia) in the northern Oklahoma City metropolitan area (OCMA) during FY97 under the STATEMAP program (Fig. 1). STATEMAP is funded by the U.S. Geological Survey and state geological surveys and is designed to provide detailed geologic mapping in high-priority need areas such as OCMA. The coauthors began this 1:24,000-scale mapping in the fall of 1997 and completed the work in the spring of 1998.

One of the objectives of the new OGS mapping project was to clarify the stratigraphic nomenclature of the various rock units in the study area. Three Permian formations are mappable in the four-quadrangle area.

The oldest formation (Wellington) crops out only in the easternmost quadrangle (Arcadia). The Wellington typically is a fine- to very fine grained, moderate orange pink to pale reddish brown and light greenish gray, color-banded sandstone with shale, siltstone, and minor conglomerate beds. Sedimentary structures include large- and small-scale crossbeds, locally steeply inclined stratification, and less-common channel-form features.

The overlying Garber Formation is similar in appearance to the Wellington but is generally coarser grained (mostly fine- to medium-grained) and tends to be reddish brown in color. A mappable shale between 15 and 30 ft thick at the top of the Wellington separates the two formations. The Garber contains minor sandstone- and siltstone-pebble conglomerate and/or breccia, dolomite conglomerate and/or breccia, siltstone, and shale. Channel-form deposits are common and paleosol horizons are present—the most noteworthy occurring at the contact with the Wellington Formation.

The Hennessey Formation conformably overlies the Garber Formation. It is predominantly a reddish brown silty shale with common light greenish gray iron-reduction spots as large as 4 in. in diameter. It contains minor siltstone and very fine grained sandstone beds that are typically cross-bedded and ripple-marked. The Hennessey includes a mappable 2- to 35-ft-thick, very fine grained, light brown to moderate reddish brown sandstone (Reeding sandstone bed) near the western edge of the Piedmont quadrangle. The overlying shale unit is mapped as the Cedar Hills Member of the Hennessey Formation, because it is similar in appearance to the shales underlying the Reeding sandstone.

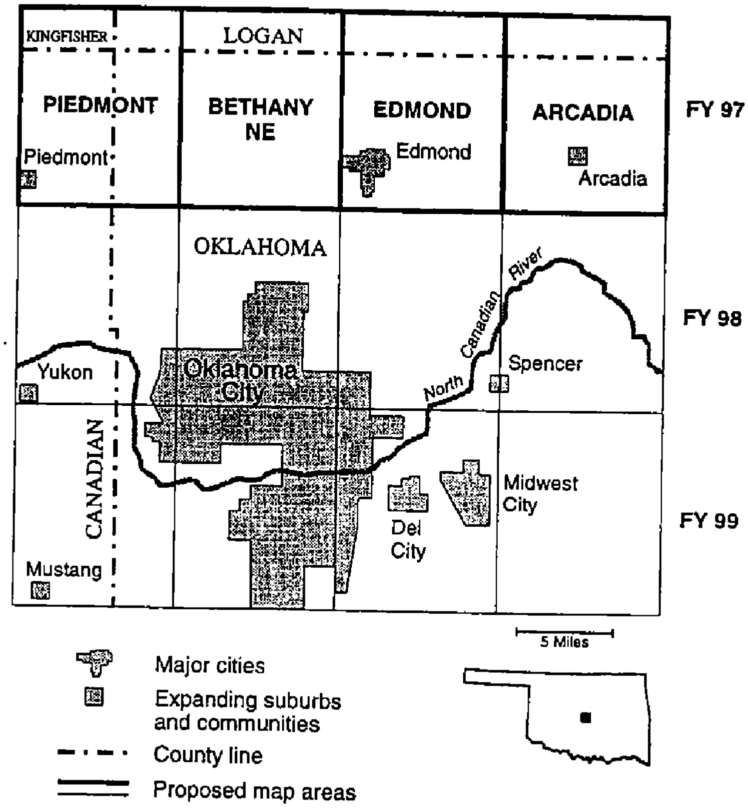

Figure 1 *(right)*. Map of the Oklahoma City Metro Area (OCMA) showing 7.5-minute quadrangles mapped in FY97 and areas to be mapped in subsequent years.

Paired Granites: Further Evidence from the Wichita Mountains, Oklahoma

JONATHAN D. PRICE and *M. CHARLES GILBERT*, School of Geology and Geophysics, University of Oklahoma, Norman, OK 73019; and *JOHN P. HOGAN*, Dept. of Geology, University of Missouri—Rolla, Rolla, MO 65409

Recent investigation has further refined the term "paired granites" to mean two or more distinct granite bodies that are contiguous, coeval, and consanguineous. Paired granites are individual bodies emplaced at the same crustal level, indicative of near simultaneous intrusion and magmatic interaction. They express subtle, relatable differences in mineral and chemical composition. Sheet granites emplaced in extensional terranes should be reviewed for possible paired granite relationships.

Two members of the Cambrian Wichita Granite Group, the Mount Scott Granite and the Rush Lake granite (formerly Unit B granite), are paired granites. These two granites result from related magmas intruding the same level of the crust at nearly the same time. Continuous contacts between these two units are observed: the westernmost exposures of the Rush Lake granite are found directly beneath the Mount Scott Granite, and eastern exposures have both granites at the same elevation, sharing near-vertical contacts. Contacts are gradational in places, sharp in others, and the sharp boundaries are commonly intimate, convoluted and swirled, indicating that both were simultaneously molten and not separated by much time. Both are alkali-feldspar granites that are porphyritic and contain variable amounts of granophyre, but there are significant differences: feldspar phenocrysts within the Mount Scott Granite are gray and ovoid, and exhibit rapakivi texture, while those within the Rush Lake granite are largely euhedral. The Mount Scott Granite also contains a higher percentage of hornblende and biotite, and it alone has magmatic plagioclase. These variations, and the corresponding differences in chemical composition, result from minor amounts of fractionation of the precursor Mount Scott Granite magma to produce the related Rush Lake granite. Major-element modeling indicates that the Rush Lake Granite is produced through crystallization of amphibole, plagioclase, and titanite from a magma of Mount Scott Granite composition. Trace-element ratios, particularly Y/La and Ba/Sr, show variation with Rb consistent with the major-element model.

In this case, differentiation occurred at a crustal magma trap, when the parental magma ponded, crystallized, and separated the fractionated phases, producing the magma that gave rise to the Rush Lake Granite. Differentiation may have been enhanced through ascent. The rise and intrusion of the Rush Lake granite provided a heated pathway for the slightly later rise of the Mount Scott Granite, resulting in the development of rapakivi texture within the latter.

Titanite-Fluorite Stability: Fluorine Content of the Mount Scott Magma

JONATHAN D. PRICE, M. CHARLES GILBERT, DAVID LONDON,
and *GEORGE B. MORGAN VI,* School of Geology and Geophysics,
University of Oklahoma, Norman, OK 73019; and *JOHN P. HOGAN,*
Dept. of Geology, University of Missouri—Rolla, Rolla, MO 65409

Experimental evaluation of titanite and fluorite stability in melt at T = 850° C, P = 200 MPa, $fO2 \approx$ NNO as functions of total F and H_2O content were assessed using the metaluminous Mount Scott Granite of the Wichita Igneous Province, Oklahoma. With no added H_2O, the granite underwent dehydration melting through biotite breakdown. Over a large range of added H_2O ($\approx$1–7 wt.%), melts containing less than 1 wt.% F precipitated titanite without fluorite, whereas melts containing greater than 1 wt.% F precipitated fluorite without titanite. Additionally, at high F ($\geq$1.2 wt.%) plagioclase and hornblende reacted to form biotite. Thus, an increase in F during crystallization may explain the increased modal abundance of plagioclase and hornblende in titanite-dominant samples of the Mount Scott Granite pluton, versus biotite in fluorite-dominant samples. Coexistence of magmatic titanite and fluorite in the Mount Scott Granite implies F_m of $\approx$1 wt.% at the early point in its crystallization history where these minerals coprecipitated. We suggest that the stability of these two phases is useful in determining the initial fluorine content in other igneous rocks: the presence of primary fluorite within high-T, shallow, moderate fO_2, subaluminous felsic rocks indicates high magmatic fluorine, whereas titanite without fluorite in such rocks indicates low initial fluorine.

Applications of Finite Element Analyses to Problems in Structural Geology

KEVIN J. SMART, School of Geology and Geophysics, University of Oklahoma, Norman, OK 73019

The finite element (FE) method is a numerical (i.e., approximate) procedure for solving problems. It can tackle complicated geometries, material properties, and applied loads for which analytical (i.e., exact) solutions cannot normally be obtained. The finite element method is common engineering disciplines, but has been more slowly applied to geological investigations because of the need to develop significant quantitative skills. For problems in structural geology, a primary advantage of the finite element method is that the complete deformation history (both stresses and strains) can be obtained.

Discretization is a fundamental approach of the FE method and involves dividing the problem into a number of elemental regions to produce the initial finite element mesh. An approximate solution to a geological problem is determined for each element. Two studies that employed this approach to analyze problems in structural geology are presented.

In the first case study, a series of finite element analyses were developed to analyze the near-surface accelerations produced by an earthquake occurring on a listric normal fault. The effects of variations in source size and hypocenter depth were evaluated. These models demonstrated that: (1) near-surface and ground accelerations from normal-fault earthquakes are controlled by both subsurface fault geometry and hypocenter depth; (2) in contrast to common wisdom, near-surface accelerations are not significantly less, and may be greater, than surface accelerations.

In the second case study, finite element models were used to assess the mechanical response to propagation and displacement of blind thrust faults. Model configurations were developed for both thrust sheets above a horizontal décollement surface, and also for roof sequences above a blind thrust horse. The mechanical response was evaluated as a function of the strength of the thrust fault surfaces. The simulations showed that: (1) the mechanical response is partitioned between thrust translation and distortion; (2) as the décollement strength increases, the ratio of distortion to translation increases; and (3) for all but the very strongest décollements, the propagating fault tip precedes the leading edge of distortion into the undeformed rock.